Accepted for presentation to the IESNA 2013 Annual Conference, Huntington Beach, CA, October 26-29, 2013 and for publication in Leukos, the journal of the IESNA.

Empirical assessment of a prismatic daylight-redirecting window film in a full-scale office testbed

Anothai Thanachareonkit, Eleanor S. Lee, Andrew McNeil

Building Technologies and Urban Systems Department, Environmental Energy Technologies Division, Lawrence Berkeley National Laboratory, Mailstop 90-3111, 1 Cyclotron Road, Berkeley, CA 94720 USA

Abstract

Daylight redirecting systems with vertical windows have the potential to offset lighting energy use in deep perimeter zones. Microstructured prismatic window films can be manufactured using low-cost, roll-to-roll fabrication methods and adhered to the inside surface of existing windows as a retrofit measure or installed as a replacement insulating glass unit in the clerestory portion of the window wall. A clear film patterned with linear, 50-250 micrometer high, four-sided asymmetrical prisms was fabricated and installed in the south-facing, clerestory low-e, clear glazed windows of a full-scale testbed facility. Views through the film were distorted. The film was evaluated in a sunny climate over a two-year period to gauge daylighting and visual comfort performance. The daylighting aperture was small (window-to-wall ratio of 0.18) and the lower windows were blocked off to isolate the evaluation to the window film. Workplane illuminance measurements were made in the 4.6 m (15 ft) deep room furnished as a private office. Analysis of discomfort glare was conducted using high dynamic range imaging coupled with the *evalglare* software tool, which computes the daylight glare probability and other metrics used to evaluate visual discomfort.

The window film was found to result in perceptible levels of discomfort glare on clear sunny days from the most conservative view point in the rear of the room looking toward the window. Daylight illuminance levels at the rear of the room were significantly increased above the reference window condition, which was defined as the same glazed clerestory window but with an interior Venetian blind (slat angle set to the cut-off angle), for the equinox to winter solstice period on clear sunny days. For partly cloudy and overcast sky conditions, daylight levels were improved slightly. To reduce glare, the daylighting film was coupled with a diffusing film in an insulating glazing unit. The diffusing film retained the directionality of the redirected light spreading it within a small range of outgoing angles. This solution was found to reduce glare to imperceptible levels while retaining for the most part the illuminance levels achieved solely by the daylighting film.

Keywords: Daylighting; prismatic film; microstructure film; windows; building energy efficiency.

---

1. Introduction

In 2010, electric lighting energy use is estimated to account for 5.42 quad (quadrillion = 10^{15} Btu) or 13% of total primary US building energy use (D&R International, Ltd. 2012). For the commercial building sector, lighting is estimated to account for 3.69 quad of which, it is estimated that 2.21 quad is associated with electric lighting use in perimeter zones located 0-12.2 (0-40 ft) from the building façade during typical daytime work hours (8:00-18:00), excluding non-applicable floor space such as religious worship or vacant space (Shehabi et al. 2013). With the introduction of useful daylight to perimeter zones, lighting energy use and associated carbon emissions can be reduced. Peak summer demand can be reduced when daylight availability is at its greatest, reducing loads on stressed utility grids.

The challenge is that conventional windows cannot provide useful daylight beyond about 1.0-1.5 times the head height of the window. Occupants lower shades over the windows to control direct sun and glare, reducing daylight, then forget to adjust the shades (often for weeks or even months) when the source of discomfort is no longer present. Daylight redirecting technologies take the approach of increasing illuminance further from vertical windows by redirecting sunlight towards the ceiling plane (Ruck et al. 2000). The daylight aperture is typically located in the upper clerestory portion of the window wall, with the lower edge of this aperture located above standing eye height or about 2 m (6.5 ft) above the finished floor. This location avoids redirecting light into the eyes of the occupants seated near the window. A separate, lower window provides seated occupants with access to outdoor views and also serves to daylight the area near the window.

There are numerous strategies for the upper aperture that have been developed and used in buildings over the decades. For the conventional light shelf, sunlight is reflected off the light shelf but for low sun angles, specularly transmitted, uncontrolled sunlight can cause glare unless a shade is lowered over the window. Daylighting systems that have near-Lambertian, diffusing properties, such as acid-etched glass or translucent panels, send incident light upwards as well as downwards to daylight the perimeter zone, but the backlit panel itself and downward daylight can also cause glare. Lowering the transmittance of the system can reduce glare but this also reduces daylight output. Reflective, mirrored louver systems address direct source glare issues by obstructing direct views of the window and redirecting sunlight upwards (for example, Bartenbach (Bartenbach et al. 1987; Beltrán et al.1997), LightLouver, and Retrosolar). These systems can be quite efficient at sunlight redirection, but the opaque reflectors obstruct admission of daylight during cloudy and overcast periods when incident light levels are low. To date, diffractive materials such as holographic optical elements or nanostructured materials have not achieved significant redirection efficiency for a broad range of incident angles, resulting in specularly transmitted sunlight that causes glare. None of these concepts have been investigated thoroughly with the advanced modeling tools available today; further investigation is warranted to quantify the merits of each approach.

Prismatic structures have long been used to refract light for a wide range of applications, some of which are applicable to vertical windows (Wadsworth 1903; Moench et al. 1987). Like reflective systems, incident light on the prismatic structure is redirected (by refraction) to the ceiling plane for the range of incident angles for which the system has been designed but have a distinct advantage over opaque reflector systems of being able to transmit daylight during cloudy or overcast periods when there is no direct sunlight. The potential for lighting energy

savings is greater, but the prismatic structure itself and the reflected sunlight on the ceiling plane can be potential sources of glare.

Metrics for lighting quality and discomfort glare have been developed for electric lighting systems and to a lesser extent, daylighting systems. Daylight-redirecting systems act like indirect lighting systems but possess potentially some of the negative qualities of poorly designed, indirect lighting systems: there can be hot spots of high intensity light on the ceiling although potentially over a much broader area. Recommended practices for electric lighting with computer displays (IESNA 2004) limit both the angle of view and luminance of electric lighting sources in the ceiling, but lamp sources tend to be small and localized while redirected daylight affects broad areas in the room, lowering contrasts, raising overall illuminance levels and room brightness, enabling the eye to adapt. These systems also admit daylight dynamically, both in distribution and intensity, which is often perceived by occupants as a positive connection to the outdoors but may confound lighting designers trying to achieve a static, controlled quality of light and appearance in the room. Because there have been few installations of such systems in buildings, there are very limited subjective appraisals of daylight redirecting systems.

Two new developments have occurred over the past decade that now enable more systematic and accurate assessments of daylight redirecting systems: a) high dynamic range (HDR) imaging coupled with digital cameras enable the lighting industry to quantitatively capture the full range of luminances seen by the human eye (Reinhard et al. 2005), and b) a new daylight discomfort glare index was derived by the Fraunhofer Institute for Solar Energy Systems and Danish Building and Urban Research (Wienold and Christoffersen 2006) from subjective responses to conventional and daylight-redirecting shading systems in full-scale offices and physical data from HDR luminance images. Both of these developments were used in this study.

We investigate the daylighting performance of a prototype, micro-structured, prismatic film designed to redirect sunlight through vertical windows. The film was installed in the clerestory windows of 4.6 m (15 ft) deep, side-by-side, full-scale, south-facing, testbed offices and monitored under real sun and sky conditions for two years (evaluations in a deeper space will be possible in 2014 when a new laboratory becomes operational). High dynamic range imaging was used to capture room cavity luminance at 5-min intervals over this period and these images were used to evaluate potential visual discomfort, particularly at a critical viewpoint applicable to both private and open plan offices at the rear of the room looking at the window. Illuminance measurements were also made, showing the relative gains in performance compared to conventional shaded windows. Field data were collected under predominantly clear sky conditions so findings are illustrative of south-facing perimeter office zones in a sunny climate. This assessment provides some insights as to whether prismatic daylight-redirecting systems have the potential to achieve significant lighting energy savings while providing a visually-comfortable indoor environment relative to conventional shaded windows. A companion simulation study was conducted to evaluate annual performance in a deep open plan office zone (McNeil et al. 2013).

2. Methods

2.1. Experimental set-up

Experimental tests were conducted at the Advanced Windows Testbed facility located at the Lawrence Berkeley National Laboratory (LBNL) in Berkeley, California. The facility was designed to evaluate the difference in thermal, daylighting, and control system performance between various façade, lighting, and some mechanical systems under realistic weather conditions. Three identical, side-by-side test rooms were built with nearly identical building materials to imitate a commercial office environment. Each furnished test room has a reconfigurable window wall facing due south. The windows in each test room are simultaneously exposed to approximately the same interior and exterior environment so that measurements between the three rooms can be compared (Fig. 1). Details of the installation and test conditions are given in Table 1.

TABLE 1. Field test conditions.

	Phase I	**Phase II**
Test period	Dec 21, 2010 to Dec 21, 2011	Dec 21, 2011 to Dec 21, 2012
Location	Berkeley, California (latitude 37°4'N, longitude 122°1'W)	Same
Test room	3.05 x 4.57 x 3.35 m (10x15x11 ft); Room A is on east side, B is center, C is on west side of south façade.	Same
Visible reflectance	Ceiling 0.87, wall 0.87, floor 0.23	Ceiling 0.82, wall 0.65, floor 0.23
Wall & ceiling paint finish	Semi-gloss	Matte
Window configuration	Clerestory facing due south, two 1.32x0.76 m (4.35x2 ft) windows, sill height 1.98 m (6.5 ft) above floor	Same
Window to wall ratio	WWR=0.14 (assuming 3.7 m (12 ft) floor to floor height; vision area only)	Same
Glazing condition	25.4 mm (1-in.) insulating glass unit, center-of-glass Tvis=0.62	Same
Test condition	Prismatic film (P1)	P1 in Room B, Prismatic film + diffuser (P2) in Room C
Reference condition	Matte-white Venetian blind[1] in Room A, fully lowered, slat angle seasonally adjusted to block direct sun	Same
Electric lighting	Off	Same
Digital camera	Nikon 990, CCD, 2048x1536 pixels	Canon EOS 5d Mark II, CMOS, 5616x3744 pixels
Fisheye lens	Nikon fisheye, FC-E8, 183°	Sigma fisheye, 8mm F3.5, 180°
Capture rate	5-min	Same

[1] Slat angles were fixed at 58°, 12°, or 0° (angle from horizontal, outdoor edge downward) for winter, equinox, and summer periods, respectively.

Paired, same-day comparisons (simultaneous measurements) were made between the reference and test conditions over solstice-to-solstice periods to evaluate performance over the range of solar positions that occur over a year.

- Phase I measurements were made in a room painted with a high reflectance, semi-gloss, bright white paint. Low-resolution, digital cameras were positioned in two locations primarily to characterize the rear zone luminance patterns. Measurements were taken from December 21, 2010 to December 21, 2011. Other non-related tests occurred over the same time period so data were not continuous over the entire period.
- Phase II measurements were made in test rooms painted with a matte, lower reflectance, medium white paint. High-resolution, digital cameras were positioned in two different locations to measure discomfort glare at a seated location at the back of the room, facing the window and at a seated location near the window facing the west side wall. Measurements were taken from December 21, 2011 to December 21, 2012. Similar to Phase I, measurements were not continuous over the entire monitored period.

Fig. 1. Outdoor view of the LBNL windows testbed facility (Room A is on the right, B is in the center, and C is on the left).

2.2. Reference and test conditions

Two test configurations were evaluated involving a microstructured, asymmetrical, multi-sided refractive prismatic film (Padiyath et al. 2013). The film consists of an orderly array of linear protrusions between 50-250 micrometers high. Each protrusion can be described as a four-sided prism where sunlight from an incident range of 5-80° is refracted by total internal reflection (index of refraction, n=1.5). The film is manufactured using roll-to-roll processing methods (for example, embossing, extrusion, casting and curing, compression molding and injection molding) and then can be adhered to a vertical window as a retrofit or replacement measure.

The first daylight-redirecting system ("P1") consists of this film adhered to the indoor surface of a 6 mm clear PMMA acrylic sheet which was then positioned inboard of the existing clerestory glazing. The lower view windows were blocked off so that performance could be isolated to the upper daylighting window. Views of and through the daylight-redirecting glazing are shown in Fig. 2: outdoor views are blurred when looking through the film. The upper and side regions of the clerestory window were shaded by the framing system. The depth of the framing system from the indoor face of the existing glazing to the outdoor edge of the aluminum curtainwall system was 6.35 cm (2.5 in.) at the sill, jamb, and head of the window opening. The total vision area of the clerestory windows was 2.0 m^2 (21.7 ft^2) or a window-to-wall area ratio (WWR) of 0.18, assuming a 3.66 m (12 ft) floor-to-floor height. The P1 system was mounted in the west test room (Room C) during Phase I testing and in the center test room (Room B) during Phase II testing. Monitored periods when the upper windows were shaded by local obstructions were excluded from the analysis.

The second daylight-redirecting system ("P2") uses the same daylight-redirecting film and a second light diffusing film (3M Fasara™ Mat Crystal 2 SH2MACRX2) (Padiyath 2011). The daylight-redirecting film was adhered to surface #2 and a light diffusing film was adhered to surface #3 in a 3.8 cm (1.5 in.) deep, dual-pane unit consisting of two 6-mm PMMA acrylic sheets. Outdoor views were completely obscured by the diffusing film, similar to views through translucent glazing. The P2 system was positioned in the same way as the P1 system, inboard of the existing glazing. The P2 system was tested in Phase II in Room C.

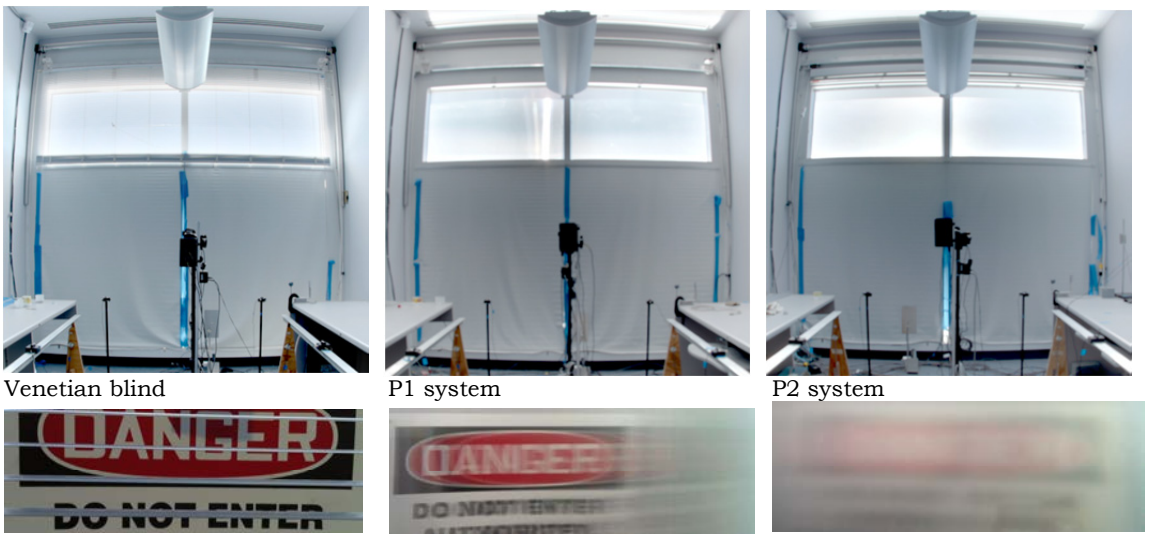

Fig. 2. Reference Venetian blind installed on the upper window with blackout shade covering the lower window with close-up of the system below (left); similar views of P1 system (middle) and P2 system (right). The outdoor object was placed within 10 cm (4 inches) from the glazing, illustrating how views are changed by the fenestration system.

The reference condition was a single 25-mm (1-in.) wide Venetian blind in a fully-lowered position covering the entire window. The slats were spaced 20 mm apart vertically and had a semi-gloss white finish on both surfaces of the slat. The reference shading system was assumed to be manually controlled by the occupant to provide comfortable work conditions

throughout the day irrespective of sky conditions. Slat angles were seasonally adjusted three times over the six-month monitored period to a cut-off angle that blocked direct sun for the majority of the day: slat angles were 58°, 12°, and 0° (angle from horizontal, outdoor edge downward, view of underside of slat from below) for winter, equinox, and summer periods, respectively.

2.3. Measured data

Indoor illuminance data and outdoor weather data were collected at a 1-min interval over a 24-h period using the National Instruments LabView data acquisition software. Indoor and outdoor horizontal and vertical illuminance measurements were made using color-corrected, cosine corrected silicon photodiodes (Li-Cor LI-210SA, ±1.5% to 150 klux) (Fig. 3). Direct normal, global horizontal, and diffuse irradiance (Hukseflux DR01, SR12, SolarTrak, ±3% of reading) were also measured. A summary of solar conditions for the days analyzed in this study is given in Table 2 and Fig. 4. All data including the following luminance data were recorded and are reported in Standard Time (ST).

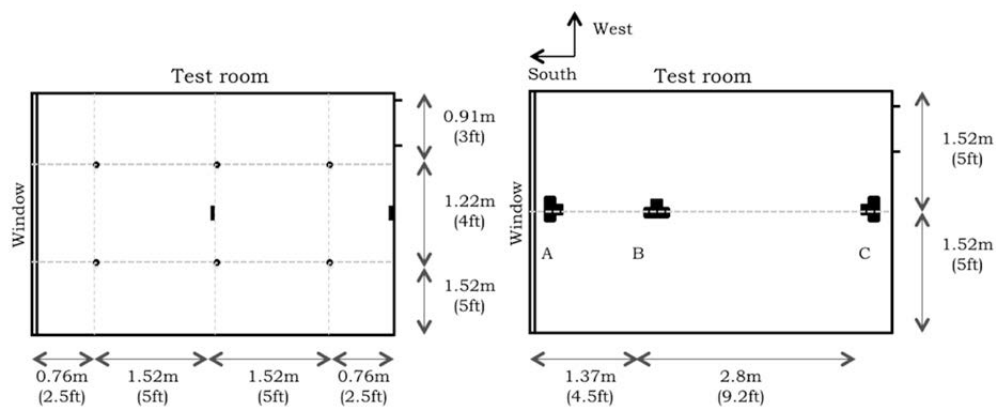

Fig 3. Location of indoor workplane illuminance sensors (left) and digital cameras (right). Phase 1: cameras A ; Phase 2: cameras B and C. A: at the window; B: 1.37 m (4.5 ft) from the window facing a computer monitor; C: 4.17 m (13.7 ft) from the window looking at the window.

TABLE 2. Outdoor solar conditions for Phase I and II test days.

	Sky type	**Solar altitude (°)**	**Global horizontal irradiance (W/m²)**		**Direct normal irradiance (W/m²)**		**Global vertical irradiance (W/m²)**	
		max	**max**	**avg**	**max**	**avg**	**max**	**avg**
Phase I								
May 12, 2011	Clear	70	976	651	900	724	422	231
April 9, 2011	Clear	59	969	569	908	676	662	351
December 3, 2011	Clear	30	534	261	915	570	980	555
Phase II								
August 20, 2012	Clear	65	898	522	794	495	517	270
October 27, 2012	Clear	40	623	330	842	560	830	486
December 19, 2012	Clear	29	497	234	869	516	970	523
August 14, 2012	Dynamic	67	1059	486	686	298	530	248
August 15, 2012	Cloudy	66	964	453	794	294	534	243
December 5, 2012	Overcast	30	194	58	5	1	107	30

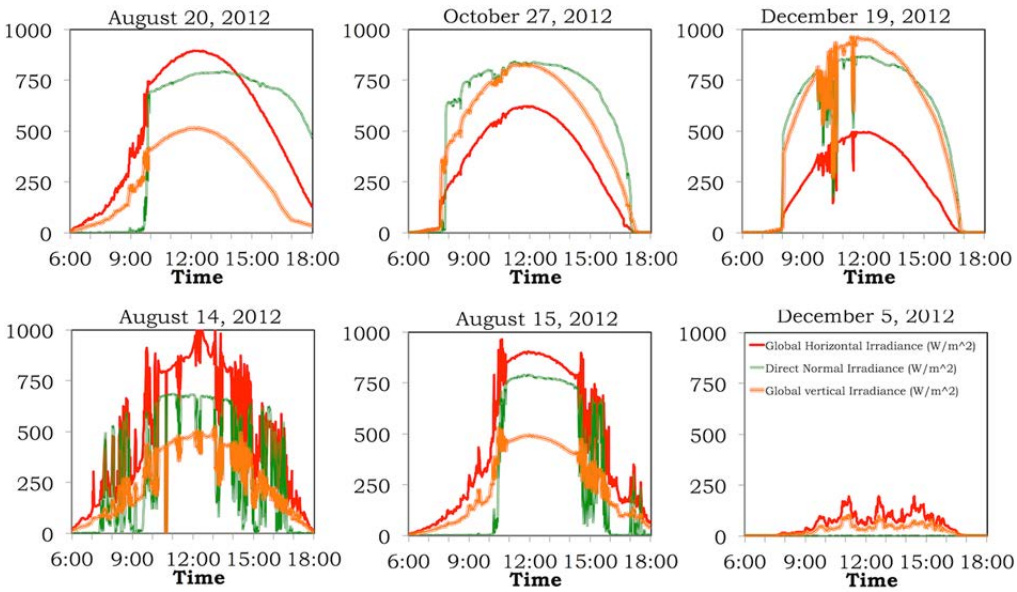

Fig. 4. Global horizontal, global vertical, and direct normal irradiance (W/m^2) for Phase II test days evaluated in this study.

Hemispherical luminance measurements were made with commercial-grade digital cameras equipped with an equidistant fisheye lens (Table 1, Fig. 3). Bracketed images (f-stop=5.6, between 4-7 images, depending on the brightness of the scene) were taken automatically (software: *hdrcaposx* (Ward 2009; Mardaljevic and Fan 2010)) at 5-min intervals from sunrise to sunset at two locations within the room interior assuming a seated occupant (1.2 m (4 ft) eye height). The low dynamic range (LDR) images were compiled into a single high dynamic range (HDR) image using the *hdrgen* tool (Ward, 2009), where the camera response function was determined by the software and the vignetting function of the fisheye lens was determined from prior laboratory tests at LBNL. A vertical illuminance measurement was taken adjacent to each camera's lens, immediately before and after the bracketed set of images, and used in the *hdrgen* compositing process to convert pixel data to photometric data. Image capture was aborted if the vertical illuminance was greater than 4000 lux for cameras facing the side wall and 14,000 lux for cameras facing the window to prevent damage to the camera's imaging sensor. A lesser number of bracketed images were taken at low light levels to avoid excessively long exposures. Analysis of discomfort glare focused on stable clear sky conditions. LDR images captured under variable sky conditions were less accurate but were retained for illustrative purposes. Luminance measurements of the six Nikon cameras were accurate to within ±5% on average under stable daylight conditions up to 11,000 cd/m^2, using a Minolta LS100 spot luminance meter and gray card as reference. The six Canon cameras used in Phase II for the glare assessments had relative errors between ±3.0% and ±5.7% (average ±4.7%) under stable daylight conditions up to 11,400 cd/m^2.

2.4. Assessment of visual discomfort

Evaluation of discomfort glare was conducted using HDR images from the digital cameras and the *evalglare* software tool (version 1.0, (Wienold 2012)). This tool identifies glare sources within a fisheye HDR image then computes various discomfort glare metrics, including the daylight glare probability (DGP) and daylight glare index (DGI), both of which are reported in this study. The DGP was derived from HDR luminance data and subjective responses from 76

people to full-scale daylit spaces, including spaces with sunlight-redirecting systems (Wienold and Christoffersen 2006). The DGP metric was independently verified as able to distinguish between "just disturbing" and "most preferable" lighting conditions in a daylit office zone by a study involving HDR luminance data and subjective responses from 18 participants (25 year old mean age) over a two day period (Van Den Wymelenberg et al. 2010). DGP calculated based on ten times the average luminance of the entire scene produced the highest correlation to survey questions. Hirning et al. (2013) however found the DGP metric to underestimate glare when the lighting conditions were dominated by contrast-based discomfort glare (low vertical illuminance) in a field study involving 63 office workers (35-60 years old). A review of discomfort glare metrics by Clear (2013) concluded that fundamental changes must be made to existing glare models, particularly in defining what exactly constitutes a glare source in a complex visual scene and how sources combine. Considerable more laboratory and field work is needed to develop and validate metrics for assessing visual discomfort for large area glare sources such as windows. Given the thoroughness of Wienold and Christoffersen's method and similarity in set up to this study, we adhered to their recommended approach in *evalglare* for the calculation of DGP. The Cornell-Hopkinson DGI formula (Hopkinson and Bradley 1960) was derived from subjective responses to artificial lighting with some later adaptations for the daylighting case and has been found to have low correlation to actual end user response to glare from daylight. It is however included in this analysis to serve as a benchmark to prior studies.

HDR images were first reduced to 799x799 pixels prior to use in *evalglare*. Arbitrarily located glare sources with a solid angle greater than 0.002 steradians (st) were identified in each image by *evalglare* using the default method: pixels with a luminance greater than the threshold luminance were identified as a potential glare source. The threshold luminance was defined as five times the average luminance within the entire 180° field of view or scene (the recommended default value given by *evalglare*). Glare source pixels were then merged into one glare source given a search radius between pixels of 0.2 steradians. Non-glare source pixels were included with glare sources if they were surrounded by a glare source (that is, smoothing option was used). Luminance peaks (>50,000 cd/m^2) were extracted as separate glare sources.

The DGP describes the probability that a person is disturbed by glare from daylight (0-1 range of values):

$$\mathrm{DGP} = c_1 E_v + c_2 \log\left(1 + \sum_i \frac{L_{s,i}^2 \omega_{s,i}}{E_v^{c_4} P_i^2}\right) + c_3 \tag{1}$$

where,
c_1=5.87x10^{-5}, c_2=9.18x10^{-2}, c_3=0.16, and c_4=1.87;
E_v = vertical illuminance at the eye (lux);
L_s = luminance of the source i (cd/m^2);
ω_s = solid angle of source i (steradians, st); and
P = position index.

Values lower than 0.2 or where the ambient light level was less than 380 lux[1] exceed the boundary conditions of the model and are considered invalid.

The DGI reports a subjective rating of the level of discomfort: values of 16, 20, 24, and 28 correspond to subjective responses of "just perceptible," "just acceptable," "just uncomfortable," and "just intolerable" glare, respectively.

3. Results

3.1. Workplane illuminance

Figure 5 illustrates the basic differences in light redirection and diffusion between the reference Venetian blind and redirecting systems P1 and P2 when conditions are clear and sunny. For a solar altitude angle of 30°, the P1 system demonstrates its ability to redirect sunlight to the ceiling plane while the P2 system provides a similar distribution but with greater diffusion of the upward redirected sunlight. A slight rainbow appearance occurs with the P1 system due to chromatic dispersion. The reference condition diffuses the sunlight, spreading daylight both upwards and downwards from the clerestory window.

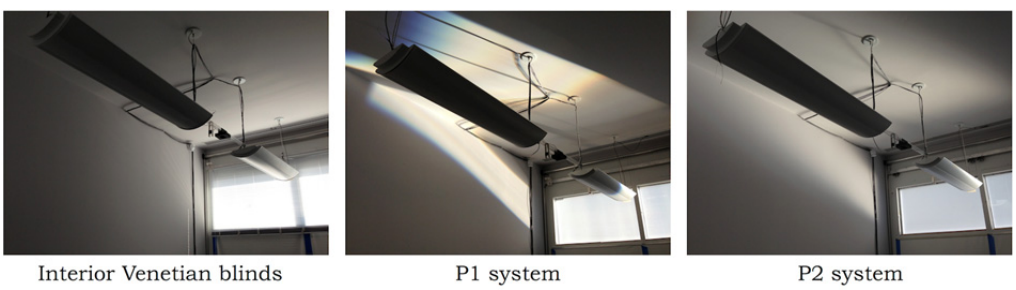

Fig. 5. Photograph of the daylight distribution resulting from the reference Venetian blind (left), P1 system (middle), and P2 system. Images are given for February 7, 2013 at 14:00 (solar altitude = 29.60°, solar surface azimuth angle = 146.3°) clear and sunny sky.

These patterns of daylight distribution are further illustrated with falsecolor luminance images in Fig. 6. Images are given for clear sky conditions at noon on days representative of the equinox and summer and winter solstice periods. The P1 system provides greatest redirection of sunlight toward the rear of the room when the solar incident angle is low (winter solstice) with the region of redirected sunlight moving closer to the window as the sun transitions to higher incident angles (summer solstice). The P2 system both diffuses and lowers the intensity of the redirected sunlight. For the equinox condition, the distribution of sunlight is similar between P1 and P2 with the area of high intensity sunlight occurring halfway across the depth of the room. For the winter solstice condition, the P2 system eliminates the high intensity area of sunlight in the rear of the room that occurs with P1, diffusing the sunlight across a broader area over the depth of the room.

[1] Wienold and Christoffersen (2006) indicated that the correlation of vertical eye illuminance to percentage of disturbed persons was expected to be valid within 1000 lux to almost 10,000 lux. For the DGP correlation, DGP was valid for DGP values greater than 0.2 and Ev greater than 380 lux (Wienold 2009).

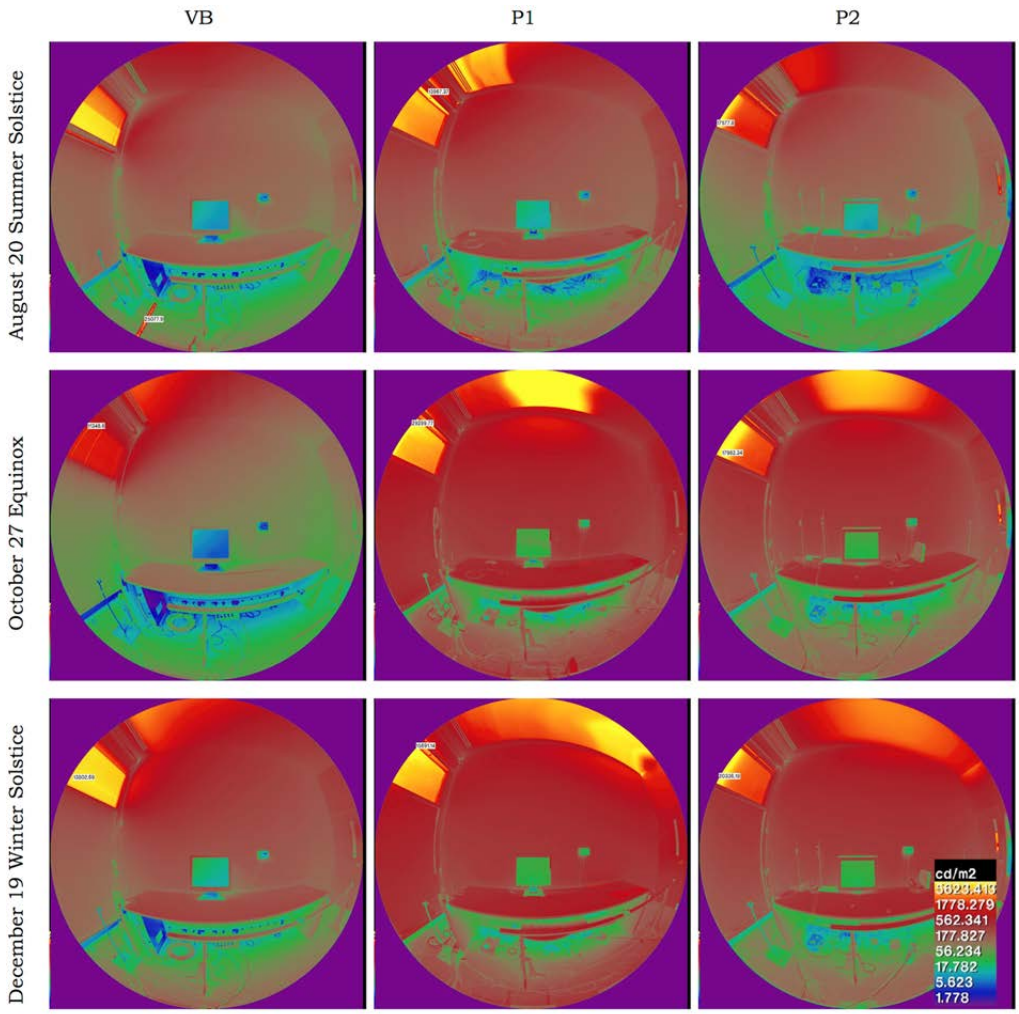

Fig. 6. Falsecolor luminance images (cd/m^2) of the test room looking toward the west side wall (window on the left) at noon on August 20, 2012 (top), October 27, 2012 (middle), and December 19, 2012 (bottom). Venetian blind (VB) (left), P1 system (middle), P2 system (right).

A second set of falsecolor luminance images are given in Fig. 7 depicting the distribution and intensity of redirected sunlight for the P1 system for a broader range of hours (8:00-12:00 Standard Time (ST)) on a clear equinox day. The images were taken from the window looking toward the back of the room. Note that the system provides no side-to-side azimuthal compensation as the sun moves from the normal plane of incidence at noon to more oblique angles: sunlight is redirected to the sidewalls of this private office. This system is designed to be used however in open plan perimeter zones with minimal vertical obstructions (that is, walls or partitions) across the width and depth of the space.

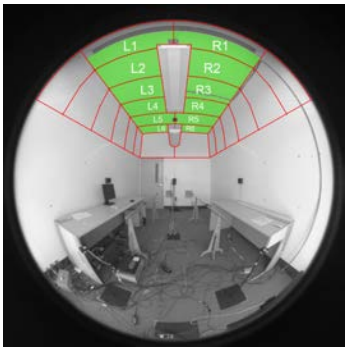

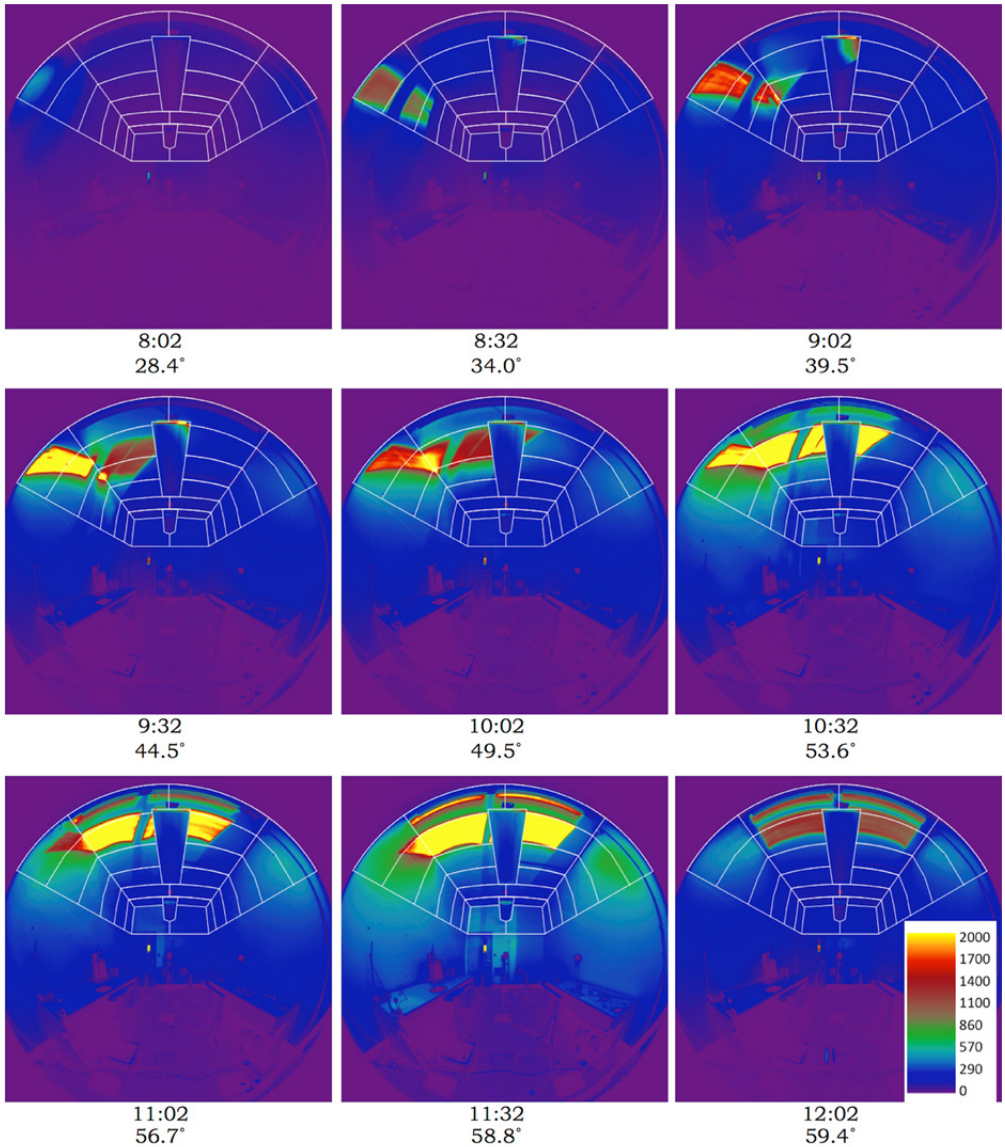

Fig. 7. Falsecolor luminance (cd/m^2) images of the test room with the P1 system on a clear equinox day, April 9, 2011, 8:00 to 12:00. Time (Standard Time) and solar altitude are given below each image. Image is for a field-of-view looking toward the rear wall of the test room. The ceiling zone area and numbering convention corresponding to Figures 8-10 is shown in the top image (L: left; R: right; zone 1 closest to window; zone 5 farthest from window). Sidewall zones were not included and are shown for visual reference only.

Similar to a light fixture, the redirected sunlight on the ceiling acts as a source that then distributes light to task surfaces. To provide a general sense of the intensity of the source, average luminance levels of the ceiling (Rvis=0.87) as a function of time of day are given in Fig. 8-10 for the P1 system (Phase I). Luminance levels are given by zone to indicate where the daylight was redirected and at what intensity. The left and right half of the ceiling were subdivided into six equal zones from the front (zone 1) to the rear (zone 6) of the room and the average luminance in each of these zones was determined from time-lapsed HDR images using a bitmap mask overlay (zones are outlined in Fig. 7). The luminance of the pendant light fixture in the center of the space and upper side walls were not included. During the summer solstice and into the equinox period, ceiling zone luminance levels nearest the window (zones 1-2) were significantly greater than the reference Venetian blind. During the winter solstice, luminance levels of the zones furthest from the window (zones 3-6) were significantly greater than the reference condition. Average ceiling zone luminance peaked at about 3500 cd/m^2 during the winter solstice in the rear of the room. Peak levels were lower during equinox and summer solstice periods, 2000 cd/m^2 and 600 cd/m^2, respectively.

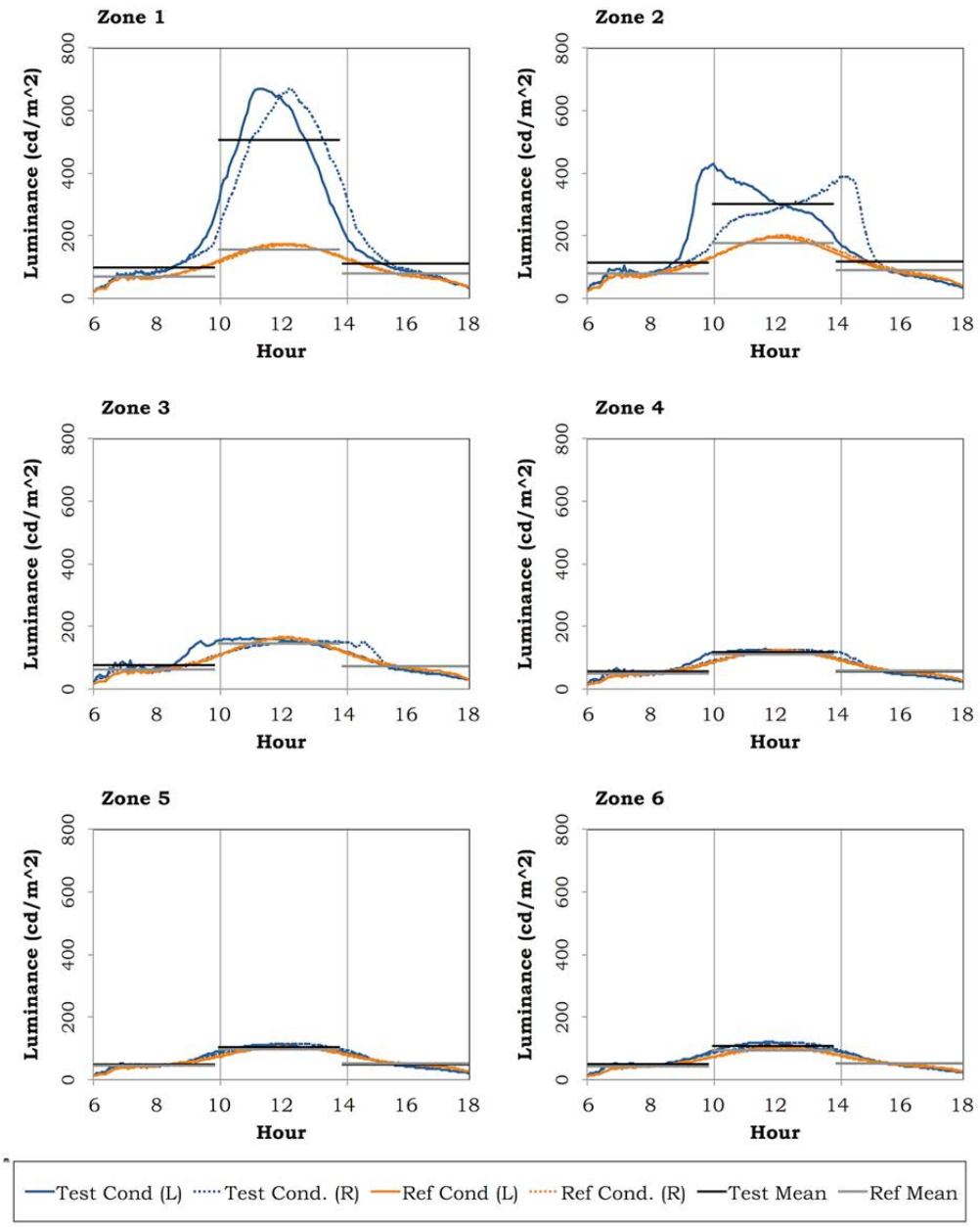

Fig. 8. Ceiling luminance by zone under clear sky conditions on May 12, 2011. Zone 1 is closer to the window and zone 6 is the farthest from the window. Phase 1, P1 system.

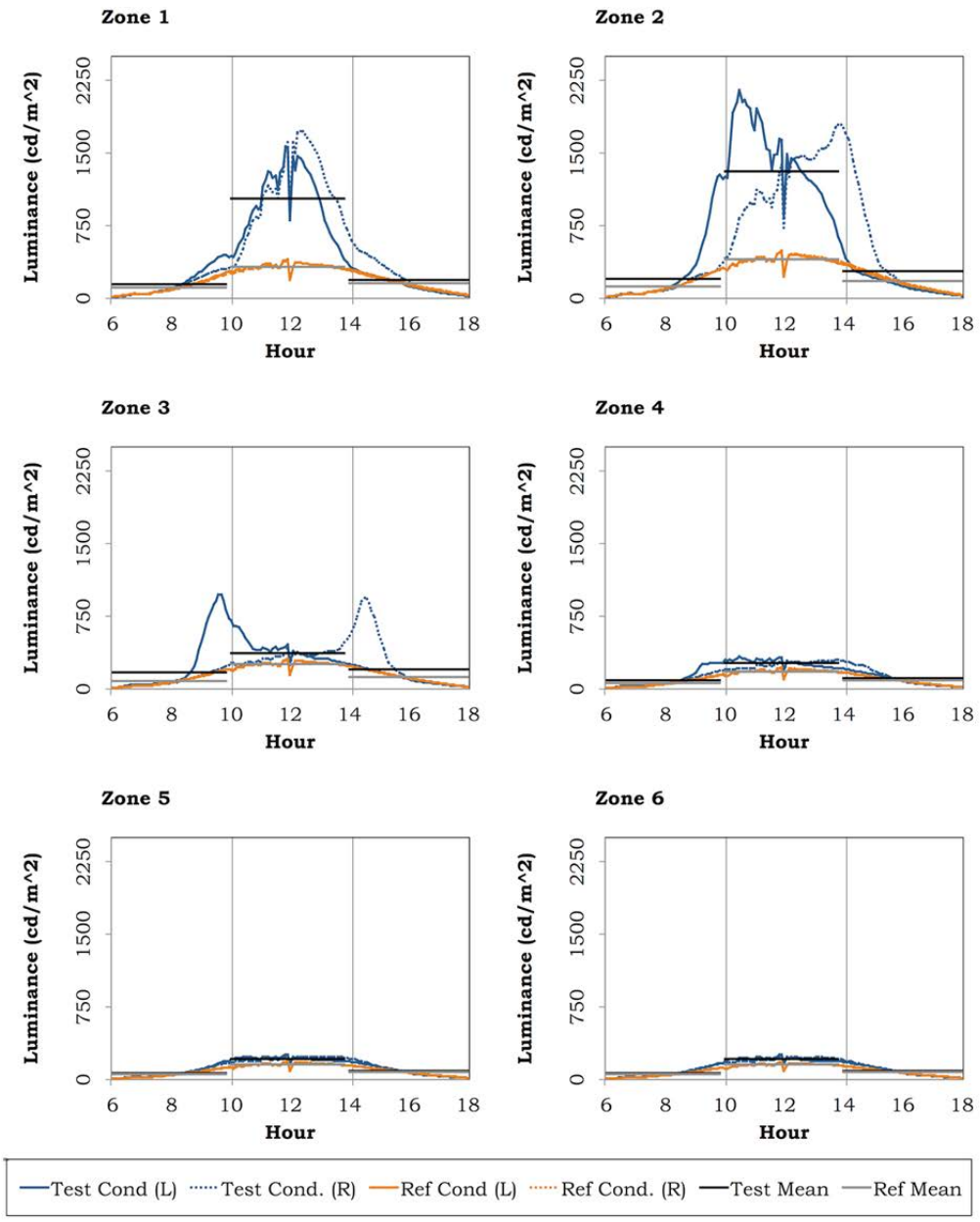

Fig. 9. Ceiling luminance by zone under clear sky conditions on April 9, 2011. Zone 1 is closer to the window and zone 6 is the farthest from the window. Phase 1, P1 system.

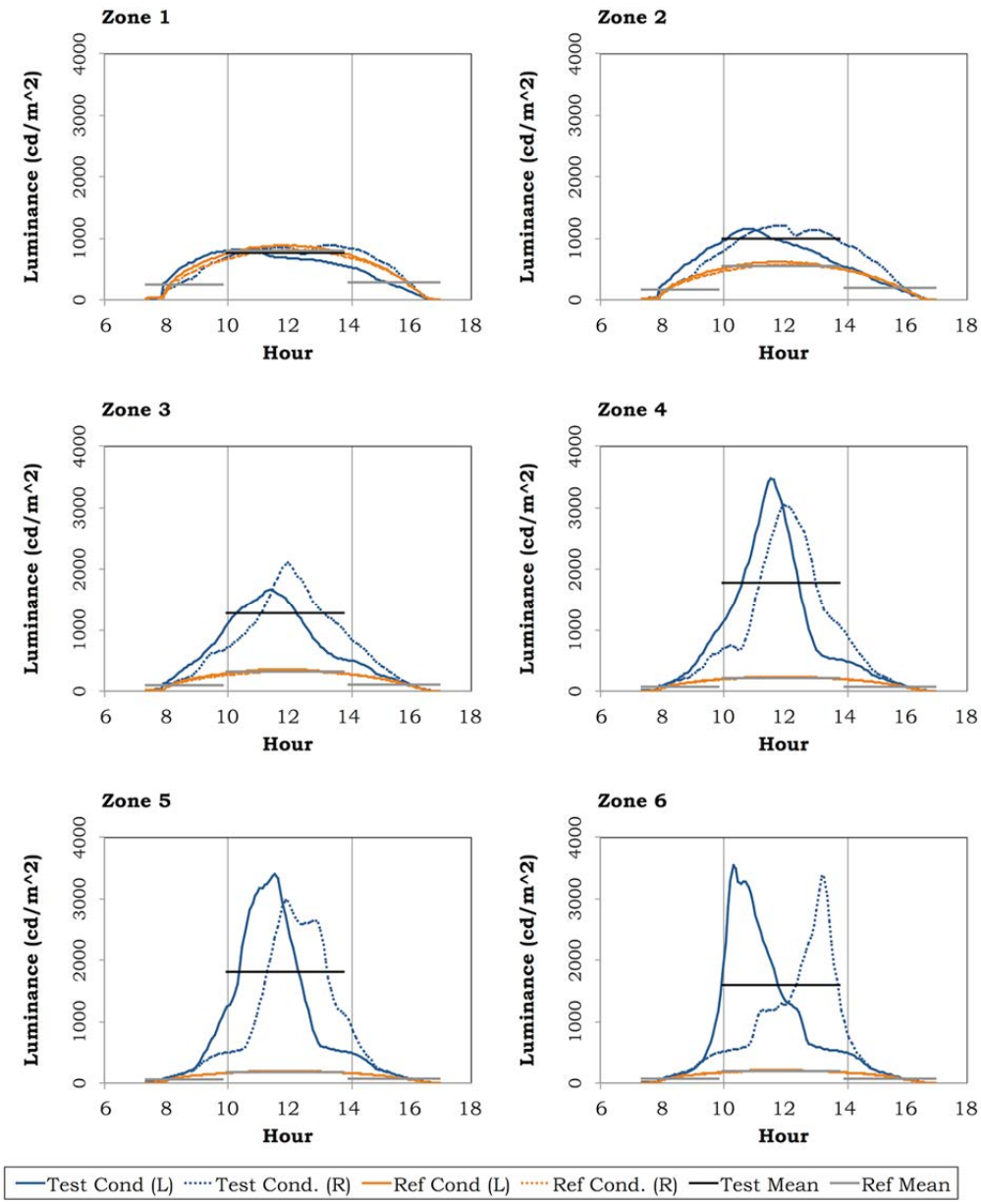

Fig. 10. Ceiling luminance by zone under clear sky conditions on December 3, 2011. Zone 1 is closer to the window and zone 6 is the farthest from the window. Phase 1, P1 system.

With the daylit ceiling as a source, we show examples of the distribution of illuminance across the depth of the space at noon on clear sunny solstice and equinox days for the reference and test cases (Fig. 11) with a sectional view of the room shown to scale. A minimum illuminance level of 500 lux is recommended by the Illuminating Engineering Society of North America (IESNA) for office tasks such as reading and writing. During the noon hour on clear sunny days when output from the daylight redirecting system was at its peak, illuminance levels were well above these recommended levels: 636-2173 lux at the rear of the room with the P2 system whereas the Venetian blind produced levels of 274-745 lux from solstice to solstice. Note that despite the 500 lux recommended level, higher, brighter levels of daylight within the entire room cavity are often welcomed by the occupants if unaccompanied by glare.

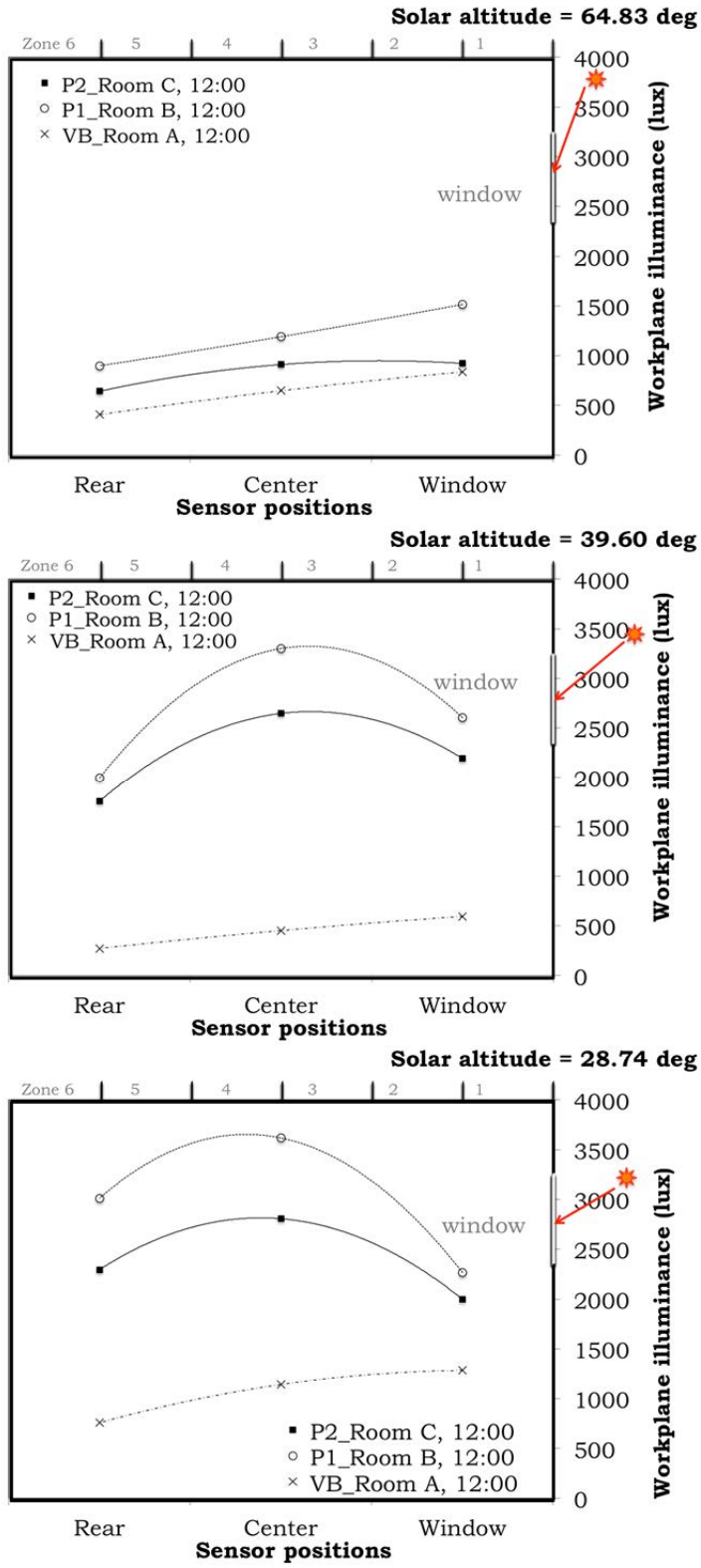

Fig. 11. Cross-section of test room showing distribution of workplane illuminance (lux) for the reference room with Venetian blinds, P1 system, and P2 system at noon on August 20, 2012 (top), October 27, 2012 (middle), and December 19, 2012 (bottom). Phase 2. Ceiling zones are shown in a cross-sectional view of the room with the window on the right and the solar altitude depicted also on the right.

Average hourly workplane illuminance levels between 6:00-18:00 ST are given for all three systems in Tables 3-4 for three clear days, one overcast day, and two dynamic sky days (Phase II). Data for the two sensors placed at the same depth from the window were averaged. We were particularly interested in increased daylight levels at the rear area of the room (above and beyond that achieved by conventional shading systems) since contributions from the lower view window will adequately illuminate work areas nearest the window. On clear sunny equinox and winter solstice days, the P1 and P2 systems provided significantly more daylight illuminance than the reference condition at the rear of the room from about 9:00 to 15:00 (Fig. 12). Illuminance levels were between 390-2173 lux with the P2 system compared to 152-745 lux with the reference shaded window. On clear sunny summer solstice days, daylight levels at the rear zone were increased from 10:00-14:00 by both systems but by a much smaller margin. When greater than the reference case, illuminance levels were between 417-636 lux with the P2 system compared to 375-405 lux with the reference window. On both dynamic days and overcast cloudy days, the P1 and P2 systems admitted more daylight than the obstructed reference window primarily between 11:00-13:00. Data are summarized in Tables 3-4.

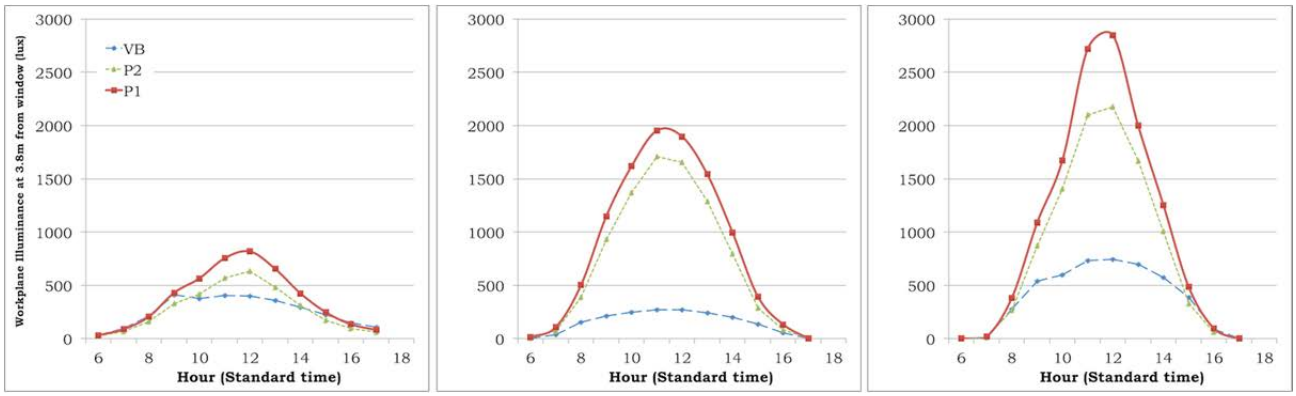

Fig. 12. Average hourly work plane illuminance at 3.8 m from the south-facing window (WWR=0.18) under clear sky conditions for summer solstice (left), equinox (right), and winter solstice days for the reference Venetian blind, P1, and P2 systems. Data are given for August 20, October 27, and December 19, 2012.

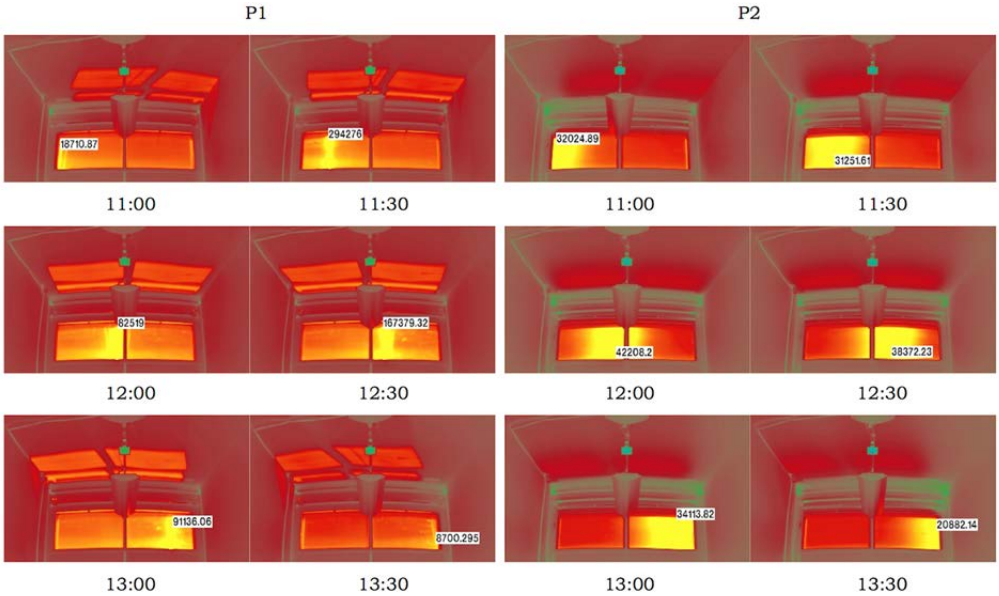

Fig. 13. Falsecolor luminance images of the window systems in the test rooms with P1 (left) and P2 (right) on a clear sunny summer solstice day, August 20, 2012. The maximum luminance in the scene is labeled on each image (cd/m^2).

TABLE 3. Workplane illuminance levels (lux) for clear sunny days.

	Illuminance (lux) at 0.76 m from window			Illuminance (lux) at 2.28 m from window			Illuminance (lux) at 3.8 m from window				
	VB	**P1**	**P2**	**VB**	**P1**	**P2**	**VB**	**P1**	**P2**	**P1-VB**	**P2-VB**
Summer solstice, August 20, 2012											
6:00	45	53	36	43	52	39	34	31	23	-3	-11
7:00	123	143	97	116	145	110	93	89	68	-4	-25
8:00	283	328	224	266	331	253	211	207	158	-3	-52
9:00	590	715	494	526	696	535	409	431	329	22	-80
10:00	738	1169	711	561	917	707	375	566	417	190	41
11:00	825	1475	854	634	1103	837	405	755	567	350	162
12:00	830	1506	910	638	1167	896	398	818	636	420	238
13:00	770	1411	773	570	973	738	357	654	479	297	122
14:00	590	918	607	452	731	563	296	425	311	129	15
15:00	382	537	342	315	429	306	226	249	175	23	-51
16:00	212	290	170	190	236	168	151	134	95	-17	-56
17:00	131	181	106	123	152	108	106	83	59	-24	-47
Equinox, October 27, 2012											
6:00	3	19	12	3	22	15	1	11	8	10	6
7:00	80	263	147	60	202	130	36	108	73	71	37
8:00	339	1223	885	251	924	704	152	503	390	351	239
9:00	474	1886	1530	357	1766	1454	215	1149	931	934	716
10:00	545	2293	1889	438	2639	2098	250	1618	1369	1369	1120
11:00	597	2620	2178	478	3304	2589	274	1953	1710	1679	1436
12:00	586	2534	2133	461	3208	2561	269	1897	1655	1628	1387
13:00	534	2165	1816	426	2455	1968	244	1543	1289	1299	1045
14:00	441	1790	1429	334	1575	1272	202	997	795	795	593
15:00	299	1048	717	226	750	532	137	397	290	260	153
16:00	119	381	194	89	247	149	54	134	83	79	28
17:00	2	9	5	2	9	5	1	4	3	3	2
Winter solstice, December 19, 2012											
6:00	0	1	1	0	1	1	0	1	1	1	1
7:00	16	36	24	14	41	27	9	21	16	12	7
8:00	509	1125	661	434	719	420	277	384	263	107	-14
9:00	954	1865	1402	833	1739	1088	541	1087	872	546	331
10:00	1030	1920	1589	912	2404	1571	599	1673	1407	1074	808
11:00	1246	2250	1953	1119	3509	2576	734	2719	2100	1986	1366
12:00	1261	2247	1967	1151	3609	2781	745	2848	2173	2103	1428
13:00	1171	2126	1791	1039	2787	2599	695	2000	1666	1305	971
14:00	1001	1917	1497	882	2002	1952	577	1255	1009	678	433
15:00	705	1341	808	605	897	698	388	487	332	99	-56
16:00	172	287	164	144	181	123	90	96	62	6	-29
17:00	0	1	1	0	1	1	0	1	1	0	1

TABLE 4. Workplane illuminance levels (lux) for dynamic, cloudy, and overcast sky conditions.

	Illuminance (lux) at 0.76 m from window			Illuminance (lux) at 2.28 m from window			Illuminance (lux) at 3.8 m from window				
	VB	**P1**	**P2**	**VB**	**P1**	**P2**	**VB**	**P1**	**P2**	**P1-VB**	**P2-VB**
Dynamic sky, August 14, 2012											
6:00	78	94	64	77	95	72	66	57	43	-9	-23
7:00	207	256	169	193	250	187	163	148	112	-15	-51
8:00	310	391	252	274	370	274	245	224	166	-21	-79
9:00	519	638	429	442	615	464	384	380	284	-5	-100
10:00	633	974	582	515	811	604	380	501	365	121	-15
11:00	808	1355	787	654	1082	811	463	712	532	249	70
12:00	866	1404	844	693	1167	880	483	761	588	279	106
13:00	806	1199	691	623	946	705	448	618	450	170	1
14:00	710	903	598	619	830	623	464	503	375	40	-89
15:00	443	537	349	400	495	363	310	297	219	-12	-91
16:00	309	372	242	288	346	257	227	208	154	-20	-73
17:00	118	138	93	113	140	105	92	85	64	-7	-27
Cloudy sky, August 15, 2012											
6:00	31	38	25	30	36	27	24	21	15	-3	-9
7:00	94	112	78	90	111	85	72	68	52	-4	-20
8:00	187	219	150	178	221	169	143	137	105	-6	-38
9:00	387	451	310	365	458	349	291	285	218	-6	-72
10:00	745	1026	637	613	888	669	439	566	419	127	-20
11:00	737	1360	765	568	1006	757	359	677	505	319	146
12:00	758	1389	816	588	1081	819	369	726	564	357	194
13:00	699	1286	692	541	896	669	347	608	439	261	92
14:00	658	911	594	548	778	593	391	466	346	76	-45
15:00	488	601	390	425	533	389	322	320	232	-2	-90
16:00	288	336	226	271	332	249	217	201	153	-16	-64
17:00	185	217	142	172	208	154	138	124	93	-13	-45
Overcast sky, December 5, 2012											
6:00	0	0	0	0	0	0	0	0	0	0	0
7:00	2	5	4	2	5	4	1	3	2	2	1
8:00	11	25	17	10	25	20	6	14	10	8	4
9:00	41	88	62	36	90	70	23	54	43	31	20
10:00	65	138	98	57	142	110	36	87	69	50	33
11:00	76	162	116	67	167	129	43	102	81	60	38
12:00	79	169	121	69	172	134	45	105	84	60	39
13:00	65	140	100	57	143	110	37	87	69	50	32
14:00	80	170	122	69	168	131	45	104	83	59	38
15:00	60	126	90	53	130	101	33	80	63	47	30
16:00	15	32	22	13	34	25	8	19	15	11	7
17:00	0	0	0	0	0	1	0	0	0	0	0

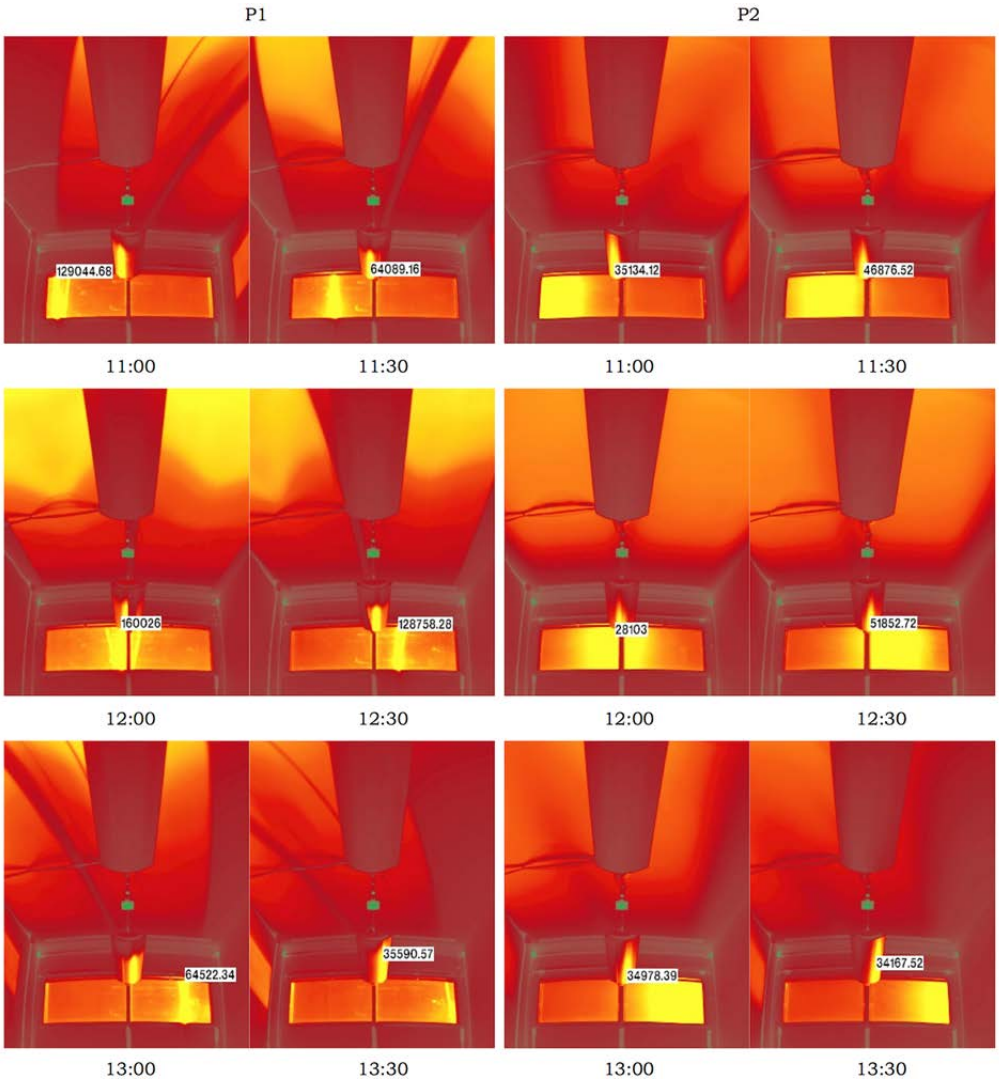

Fig. 14. Falsecolor luminance images of the window systems in the test rooms with P1 (left) and P2 (right) on a clear sunny winter solstice day, December 19, 2012. The maximum luminance in the scene is labeled on each image (cd/m^2).

3.2. Discomfort glare

The previous section's analysis focused on how daylight was distributed within the room and, with reflected daylight on the ceiling acting as a source, the resultant illuminance on the workplane. In this section, we determine whether the daylight causes visual discomfort for a seated occupant with a horizontal line of sight (assuming that the primary task is working on a computer) looking either towards the window from the rear of the room or at a position near the window looking at the sidewall. As mentioned in Section 2.4, we compared system performance using the DGP metric but also provided DGI data to serve generally as a benchmark to prior studies.

For the P1 system, the light distribution across the ceiling and wall surfaces was observed to have large areas of high intensity light tapering to regions of less intensity (Fig. 13-14). Across the window surface itself, the brightness of the window was uniform with the exception of a small region of intense brightness when the orb of the sun was within the line of sight. For the

P2 system, this small region of intense brightness was diffused across a wider area. There were no specular sources of sunlight resulting from the window system itself within the line of sight. However, if the redirected sunlight struck reflective surfaces within the room (for example, semi-reflective paint on the underside of the pendant light fixture), small-area sources of reflected light occurred within the field of view.

The *evalglare* software tool was used to detect glare sources within the field of view (Fig. 15-17). For a view position from the back of the room looking towards the window, the window was centered on the observer's line of sight with a slight upward angular displacement (position index, P_s = 1.5; solid angle of source, ω_s=0.09). With a search radius between each pixel, r, of 0.2 sr, for many of the hours of the day during the summer solstice, the window and the reflected daylight on the ceiling were combined as a single source of glare with an average luminance.[2] During the winter, the reflected light on the ceiling was distributed over a broader area further from the window and was therefore identified as a separate glare source from the window. Sources on the ceiling tended to have a high position index, indicating less discomfort compared to glare sources aligned with the line of sight to the task.

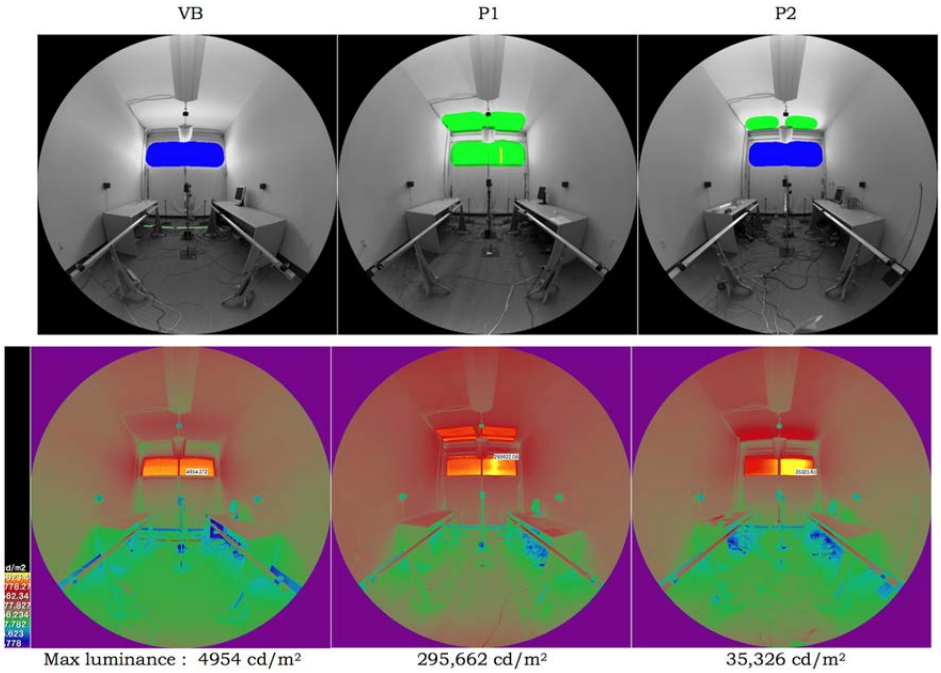

Fig. 15. *evalglare* (above) and falsecolor luminance images (below) of the reference room with Venetian blinds (left) and test rooms with P1 (middle) and P2 (right) on August 20, 2012 at 12:40. The color used in the *evalglare* images to highlight the identified glare sources is not meaningful.

[2] Wienold and Chistoffersen (2006) found no significant change in the DGP correlation for a search radius within a range of 0-0.8 sr.

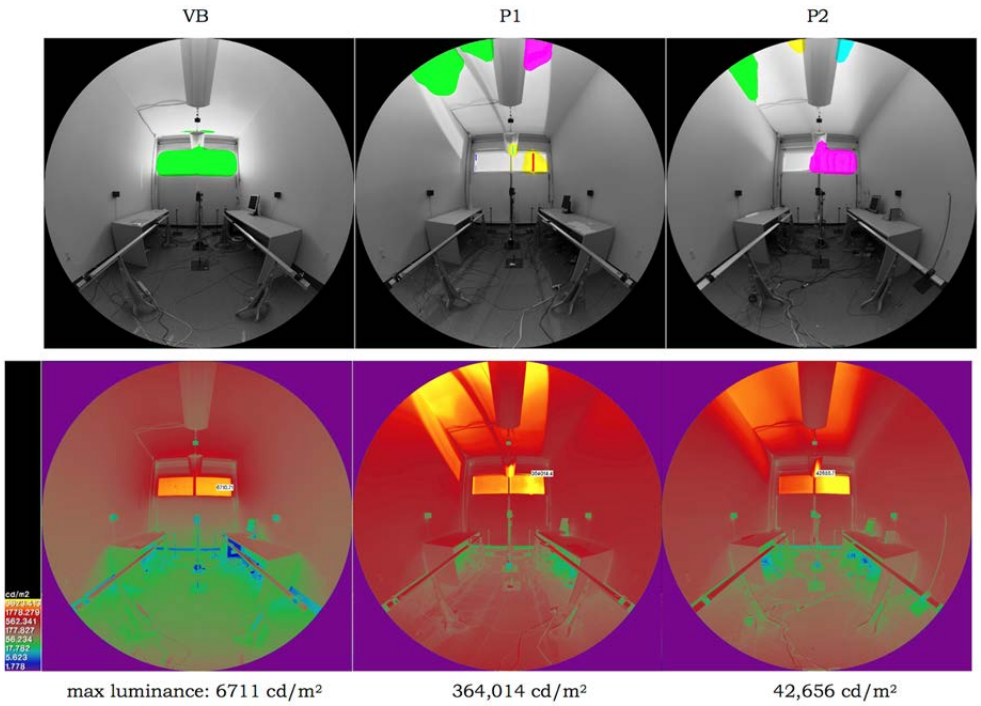

Fig. 16. *evalglare* (above) and falsecolor luminance images (below) of the reference room with Venetian blinds (left) and test rooms with P1 (middle) and P2 (right) on December 19, 2012 at 12:55. The color used in the *evalglare* images to highlight the identified glare sources is not meaningful.

Whether these sources resulted in discomfort glare is related to the vertical illuminance at the eye. The conventional background luminance, L_b, as a measure of adaptation level used in other glare formulations (for example, DGI) was found in (Wienold 2006) to be poorly correlated in the derivation of the DGP formula because large area sources affect adaptation level. Sufficient vertical illuminance at the eye can work to counteract the glare effect of large area sources (since E_v is a term in the denominator of the summation term of Equation 1). The c_1E_v term in Equation 1 contributed for example, a maximum of 0.09 and 0.20 to the total DGP value (at noon) for the P1 system on the summer and winter solstices, respectively. Note that similar to the experimental study conducted for the derivation of DGP, the electric lights were turned off in this study so vertical illuminance was due solely to daylight.

The DGP profile is plotted as a function of time of day in Fig. 18. The DGP does not reflect the magnitude of glare perceived by the observer. Instead it gets around the problem of person-to-person variability in response to perceived glare by estimating the probability that a person is "disturbed" by glare (the DGP formulation defined "disturbed" based on the subject rating the daylight glare source to be "disturbing" or "intolerable"). The time series plots in Fig. 18 show the relative differences in DGP performance where the P1 system produced DGP values between 0.30-0.45 during the core hours around noon for both the summer and winter solstice, while the P2 system produced DGP values between 0.25-0.27. The DGP was maintained around 0.20-0.22 by the reference Venetian blind. DGP values of less than 0.2 are invalid. These values are given for the most conservative position: a view looking directly at the window and ceiling glare sources from the rear of the room where vertical illuminance levels and therefore adaptation levels are at their lowest.

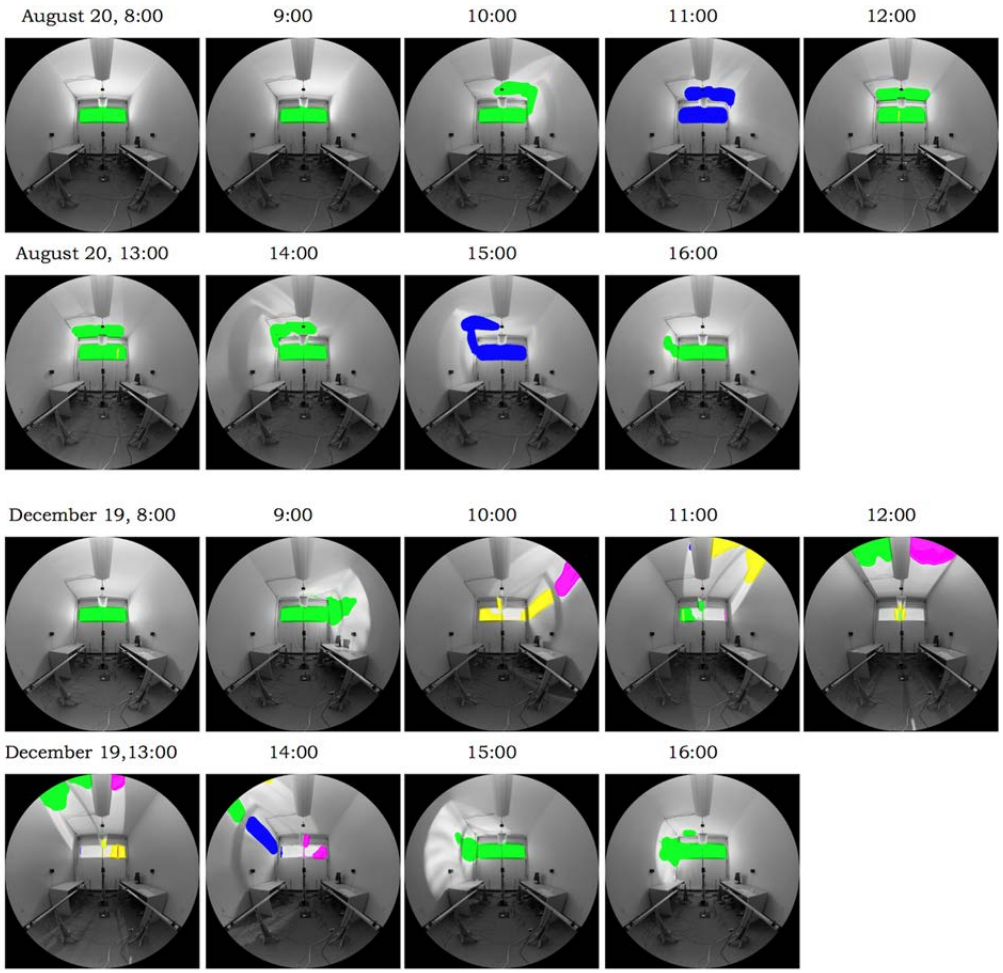

Fig. 17. Location of glare sources detected by *evalglare* for August 20, 2012 (upper two rows) and December 19, 2012 (lower two rows) for hours 8:00-16:00 ST. Sources from peak extraction are shown but are very small. Phase II, P1 system.

Wienold derived a method to account for the frequency of glare over a time period, where within a defined category of comfort, 3-5% exceedance of a threshold limit is allowed (Wienold 2009). Glare ratings ranging from "imperceptible" to "intolerable" were first related to DGP values in a descriptive one-way analysis of the study's user assessment data, then various categories or classes of comfort were defined:

- Class A or "best" class: 95% of the time period DGP must be less than or equal to 0.35 ("imperceptible" glare) and the remaining 5% of the time must have an average DGP limit of 0.38 ("perceptible" glare).
- Class B or "good" class: 95% of the time period DGP must be less than or equal to 0.40 ("perceptible" glare) and the remaining 5% of the time must have an average DGP limit of 0.42 ("disturbing" glare).
- Class C or "reasonable" class: 95% of the time period DGP must be less than or equal to 0.45 ("disturbing" glare) and the remaining 5% of the time must have an average DGP limit of 0.53 ("intolerable" glare).

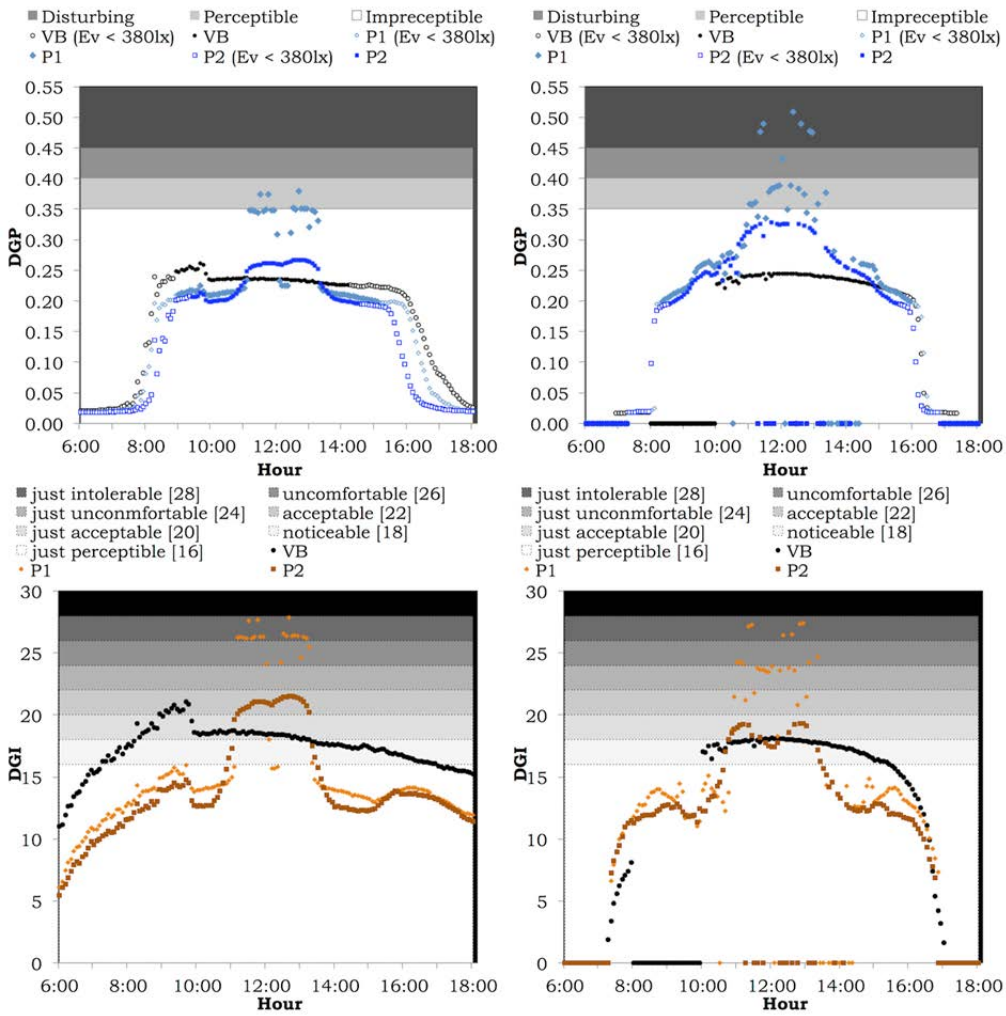

Fig. 18. Daylight glare probability (DGP, upper) and daylight glare index (DGI, lower) versus time of day computed using *evalglare* for three systems (VB, P1 and P2), August 20, 2012 (left), December 19, 2012 (right). View from the rear of the room looking at the window.

These classes were calculated for each measured day over a period from 8:00-18:00 ST (which included a maximum of 1.5 h of data when the sun had set during the winter). For a clear sunny day during the summer solstice with a view from the rear of the room looking towards the window (Fig. 18), all three systems satisfy the Class A criteria of imperceptible glare. For a clear sunny day during the winter solstice, the P1 system falls into the Class C category of disturbing glare while the P2 and reference systems remain in the Class A category. For the same periods but with a view near the window looking at the sidewall (Fig. 19), all three systems again fall into the Class A category of imperceptible glare during the summer solstice. For a clear sunny day during the winter solstice, the P1 system falls into the Class B category of perceptible glare while the P2 and reference systems remain in the Class A category. The vertical illuminance levels are greater in this area. For example, the c_1E_v term contributed a maximum of 0.045 and 0.15 to the total DGP value for the P1 system on the summer and winter solstices, respectively. The glare sources also have position factors that are outside the primary line of sight. During early morning and late afternoon winter hours, one can see in Fig. 17 downward redirected sunlight on the side walls of the test room when sunlight was at

an oblique angle to the window. Notice, however, that *evalglare* did not identify these patterns of light as glare sources.

The same method of analysis was applied to all clear sunny days over the Phase II monitored period then summarized in Fig. 20. The average DGP for the 5% period is plotted as a point on the graph as a function of the maximum solar altitude for each day analyzed. For the whiskers or dispersion associated with each point, the maximum DGP value for the 95% period is shown as the lower edge of the range and the maximum DGP value for the whole time period is shown as the upper edge. The resultant classes are summarized in Table 5. For the high summer angles (maximum solar altitude between 55-70°), the reference Venetian blind and P2 system consistently perform within the Class A requirements whereas the P1system just fails the Class A requirements – the 5% criterion is met but not the 95% criterion for all but a few days near the summer solstice. The P1 system falls into the Class C category during winter periods when the sun angle is low while P2 and the Venetian blind remain in Class A.

TABLE 5. Daylight glare probability (DGP) Class for clear sunny days, 8:00-18:00 ST.

Date	Max solar altitude (°)	Reference Venetian Blind				P1 System				P2 System			
		Max DGP 95%	Mean DGP 5%	Max DGP	Class	Max DGP 95%	Mean DGP 5%	Max DGP	Class	Max DGP 95%	Mean DGP 5%	Max DGP	Class
7-Dec-12	29	0.24	0.24	0.25	A	0.39	0.47	0.50	C	0.32	0.33	0.33	A
19-Dec-12	30	0.24	0.24	0.25	A	0.43	0.49	0.51	C	0.33	0.33	0.33	A
12-Nov-12	35	0.20	0.20	0.20	A	0.40	0.41	0.42	B	0.32	0.32	0.32	A
28-Oct-12	40	0.19	0.19	0.19	A	0.37	0.38	0.40	B	0.30	0.30	0.30	A
27-Oct-12	40	0.19	0.19	0.19	A	0.37	0.38	0.40	B	0.30	0.30	0.30	A
17-Sep-12	54	0.25	0.25	0.26	A					0.26	0.26	0.26	A
12-Sep-12	56	0.24	0.25	0.25	A	0.36	0.38	0.39	B	0.26	0.26	0.27	A
11-Sep-12	57	0.24	0.24	0.24	A	0.36	0.38	0.39	B	0.27	0.27	0.27	A
10-Sep-12	57	0.24	0.24	0.24	A	0.36	0.38	0.39	B	0.27	0.27	0.27	A
9-Sep-12	57	0.23	0.24	0.24	A	0.36	0.39	0.40	B	0.27	0.28	0.28	A
7-Sep-12	58	0.24	0.24	0.24	A	0.39	0.39	0.40	B	0.28	0.28	0.29	A
4-Sep-12	59	0.23	0.23	0.23	A	0.36	0.39	0.39	B	0.28	0.28	0.29	A
3-Sep-12	60	0.23	0.23	0.23	A	0.36	0.39	0.39	B	0.28	0.28	0.29	A
30-Aug-12	61	0.23	0.23	0.23	A	0.35	0.37	0.38	B	0.28	0.28	0.28	A
28-Aug-12	62	0.23	0.23	0.23	A	0.35	0.37	0.38	B	0.27	0.28	0.28	A
27-Aug-12	63	0.23	0.23	0.23	A	0.35	0.36	0.38	B	0.27	0.28	0.28	A
20-Aug-12	65	0.25	0.26	0.26	A	0.35	0.36	0.38	A	0.26	0.27	0.27	A
12-Aug-12	67	0.24	0.24	0.24	A	0.34	0.35	0.37	A	0.26	0.26	0.26	A
10-Aug-12	68	0.23	0.23	0.23	A	0.34	0.35	0.37	A	0.26	0.26	0.26	A

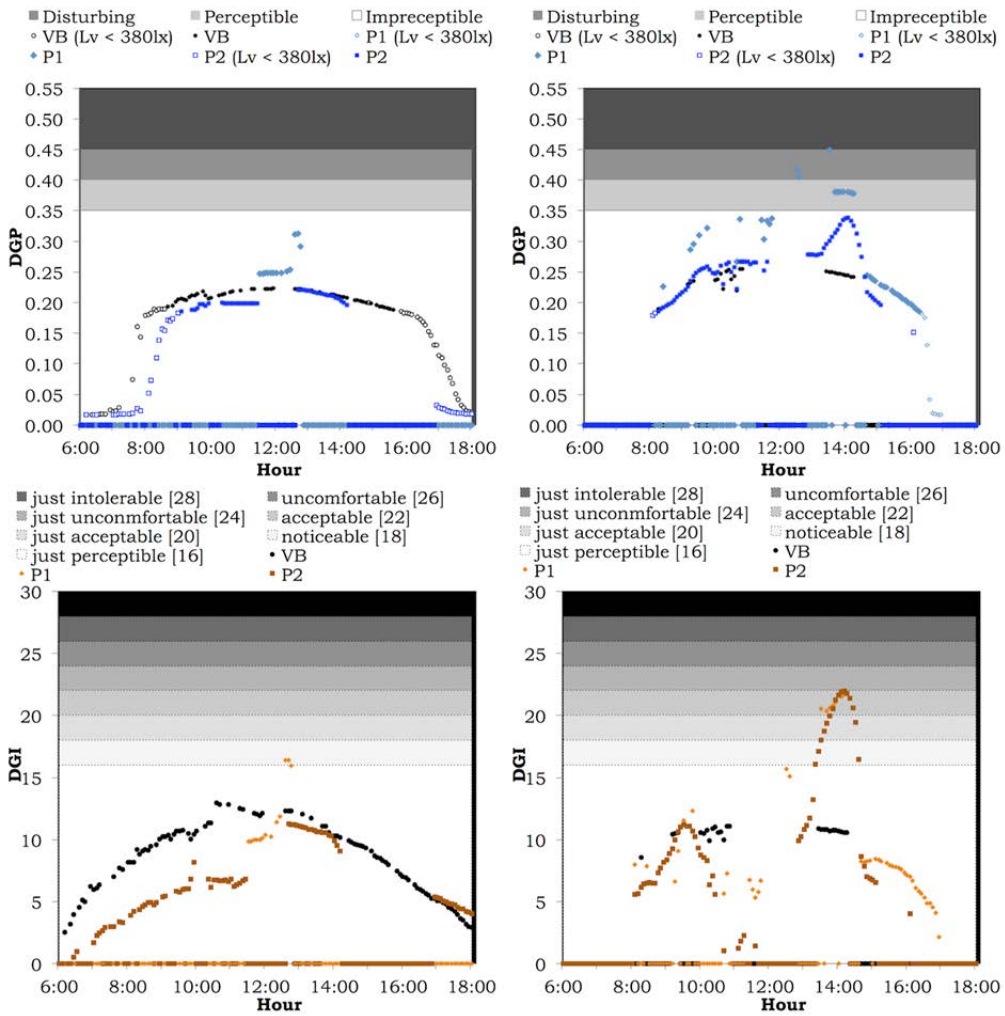

Fig. 19. Daylight glare probability (DGP, upper) and daylight glare index (DGI, lower) versus time of day computed using *evalglare* for three systems (VB, P1 and P2), August 20, 2012 (left), December 19, 2012 (right). View from near the window looking at the sidewall.

If we take four clear sunny days representative of the solar positions over the year and conduct the same analysis, we can see the distribution of DGP values for the upper 10% in Fig. 21 for the views facing the window and facing the sidewall. Summary values are given in Tables 6-7. Facing the window from the rear of the room, the P1 and P2 systems produce DGP values that are 0.25 and 0.50-0.75 greater than the Venetian blind system, respectively, until about the last 2% of the period. The P1 system produces an abrupt increase in DGP values between 0.40-0.50 (between "disturbing" and "intolerable" glare) for the remaining 2% of the period, putting it into Class B. Differences between the systems are less for the view facing the sidewall and the increase in DGP values occur in the last 0.5% for the P1 system. All three systems meet the Class A criteria. These figures confirm the trends observed above: when the path of the sun is lower in altitude (winter season), the light output from the P1 system is at its maximum enabling lesser lighting energy use, but the magnitude and frequency of discomfort glare is also greater. The P2 system significantly reduces this glare to imperceptible levels but must sacrifice lighting energy savings to do so.

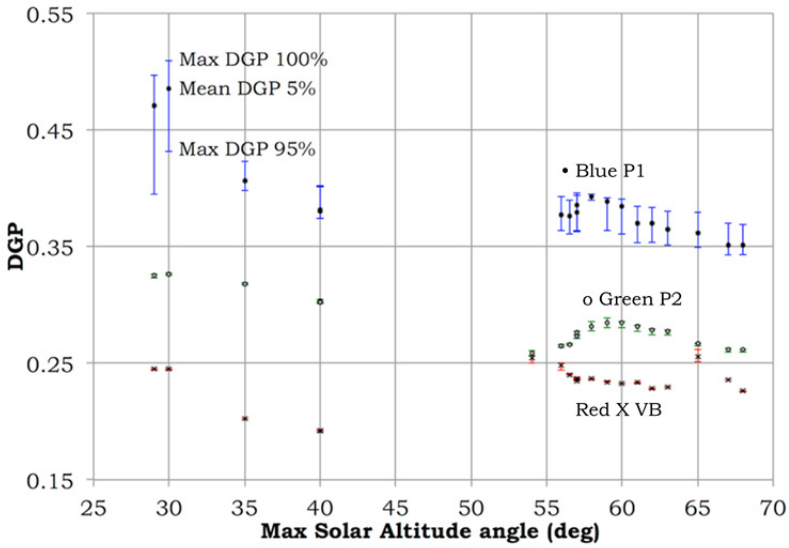

Fig. 20. Average daylight glare probability (DGP) for the 5% period on clear sunny days as a function of maximum solar altitude for each of the three systems (reference Venetian blind (VB) and the P1 and P2 systems). The range indicates the maximum DGP for 95% period (lower bound) and the maximum DGP for the entire day (upper bound). The day period was 8:00-18:00 ST.

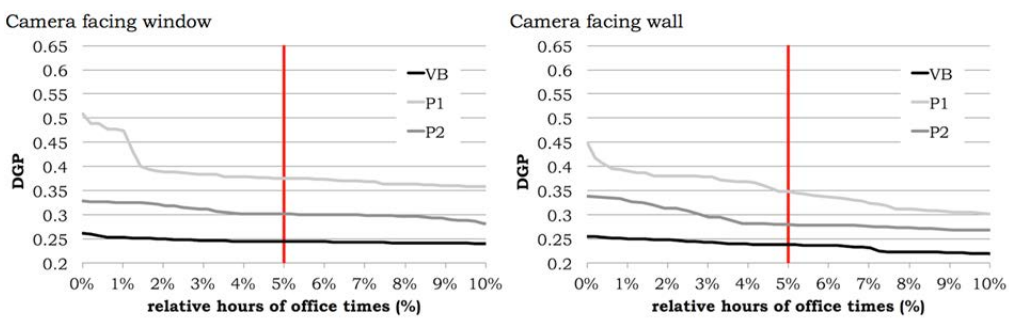

Fig. 21. Distribution of DGP values for the upper 10% of the period defined by four clear sunny days representative of solar positions over the year (December 19, October 28, September 12, August 20). Distributions are shown for each of the three systems for a seated view facing the window from the rear of the room (left) and for a seated view looking at the side wall (right). The day period was 8:00-18:00 ST.

TABLE 6.
Daylight glare probability (DGP) Class for four clear sunny days over the year, 8:00-18:00 ST, facing the window.

	Max DGP 95%	Mean DGP 5%	Class
VB	0.24	0.25	A
P1	0.37	0.39	B
P2	0.3	0.3	A

TABLE 7.
Daylight glare probability (DGP) Class for four clear sunny days over the year, 8:00-18:00 ST, facing the sidewall.

	Max DGP 95%	Mean DGP 5%	Class
VB	0.24	0.24	A
P1	0.34	0.35	A
P2	0.28	0.34	A

4. Discussion

The primary value of full-scale field measurements is that one can directly observe and measure the effects of prototype technologies under real sun and sky conditions, particularly visual discomfort which can be difficult to model using current simulation tools when systems with peaky output distributions such as the one studied here are involved.

Several summary observations can be made about the two prototype systems. The P1 prismatic film effectively redirected sunlight up towards the ceiling plane but the light was focused and caused perceptible to disturbing levels of glare to occupants seated toward the rear of the room and facing the window primarily during winter mid-day hours when the angle of incidence was low and incident vertical irradiance levels were high. When a diffusing layer was added to the system, the P2 system spread the redirected daylight over a larger area with reduced intensity; discomfort glare levels dropped to imperceptible levels. On cloudy and overcast days and for view positions that did not include the window within the direct line of sight, discomfort glare was imperceptible for both systems. During periods when the daylight was redirected towards the rear of the room, task workplane illuminance levels of both the P1 and P2 systems were significantly greater than that of a conventional interior shade – these periods occurred for the majority of daytime work hours during the equinox to winter solstice period (6 months out of the year) under clear sunny conditions.

The overall level of adaptation and therefore level of glare discomfort may have been influenced by the lack of daylight from the lower view window. A short test was conducted during the equinox period with the lower window uncovered to allow daylight admission (same glazing as the upper window, vision area of 4.5 m^2 (48.5 ft^2) or WWR=0.40). A Venetian blind was positioned over this lower window with the same slat angle as the reference room. We plotted the glare source position, size, and time of day as an overlay to a fisheye view of the side wall near the window for a clear sunny day (Fig. 22). For this time of the year, sunlight patterns were not as low on the sidewalls as those that occurred during the winter solstice; bright sunlight occurred only on the upper region of the sidewall. This case provides a more realistic depiction of the room cavity luminance levels that would occur with a clerestory and large-area lower view window (without supplementary electric lighting). The *brightest* glare sources (10,000-100,000 cd/m^2) originated from the sunlight-redirecting system itself or from reflected sunlight off the sill of the lower window. These sources were generally less than 0.1 st, with glare sources on the ceiling at 0.3 st or less. The *largest* glare sources (0.4-0.5 st) were due to the lower window with luminance levels between 1000-10,000 cd/m^2. With the lower window, vertical illuminance at the eye was pushed to levels greater than 5000 lux from 10:00-14:00 ST, contributing 0.45 or more to the total DGP value.

With the addition of glare sources from the lower window, DGP levels were raised significantly, particularly for the view looking at the sidewall (Fig. 23; Tables 8-11). For the P1 system, DGP levels were between 0.45-0.57 ("disturbing" to "intolerable") between 10:00-14:00 ST compared to DGP levels that were for the most part below 0.40 for the sidewall view without the lower window (Fig. 9). The P2 system with the lower window remained in the Class A category for the view of the window from the back of the room but fell into the Class B category for the view near the window facing the sidewall. To reduce glare, the occupant would need to select a slat angle for the lower window that is more tightly closed than the cut-off slat angle used in this test. DGP data are given in Fig. 23 for the viewpoint from the rear of the room as well –

interestingly, these values were similar to those seen in the previous analysis without the lower window with a similar relative ranking between the three systems (Fig. 18). The brightness of the lower window raised overall DGP levels but did not cause the DGP to exceed levels of 0.35 (imperceptible/ perceptible glare). This short test illustrates the difficulty of using field tests to isolate how factors like adaptation level affect the visual discomfort assessment of the sunlight-redirecting system. The lower window contributed both additional light at the eye, raising adaptation levels, but also introduced additional sources of glare.

TABLE 8.

Daylight glare probability (DGP) Class for March, 12, 2013 when the VB was installed on lower window, 8:00-18:00 ST, facing the window.

	Max DGP 95%	**Mean DGP 5%**	**Class**
VB	0.34	0.34	A
P1	0.40	0.41	B
P2			

TABLE 9.

Daylight glare probability (DGP) Class for March 12, 2013 when the VB was installed on lower window, 8:00-18:00 ST, facing the sidewall.

	Max DGP 95%	**Mean DGP 5%**	**Class**
VB	0.51	0.51	Discomfort
P1	0.55	0.56	Discomfort
P2			

TABLE 10.

Daylight glare probability (DGP) Class for March, 17, 2013 when the VB was installed on lower window, 8:00-18:00 ST, facing the window.

	Max DGP 95%	**Mean DGP 5%**	**Class**
VB	0.34	0.34	A
P1			
P2	0.35	0.35	A

TABLE 11.

Daylight glare probability (DGP) Class for March 17, 2013 when the VB was installed on lower window, 8:00-18:00 ST, facing the sidewall.

	Max DGP 95%	**Mean DGP 5%**	**Class**
VB	0.48	0.49	Discomfort
P1			
P2	0.38	0.38	B

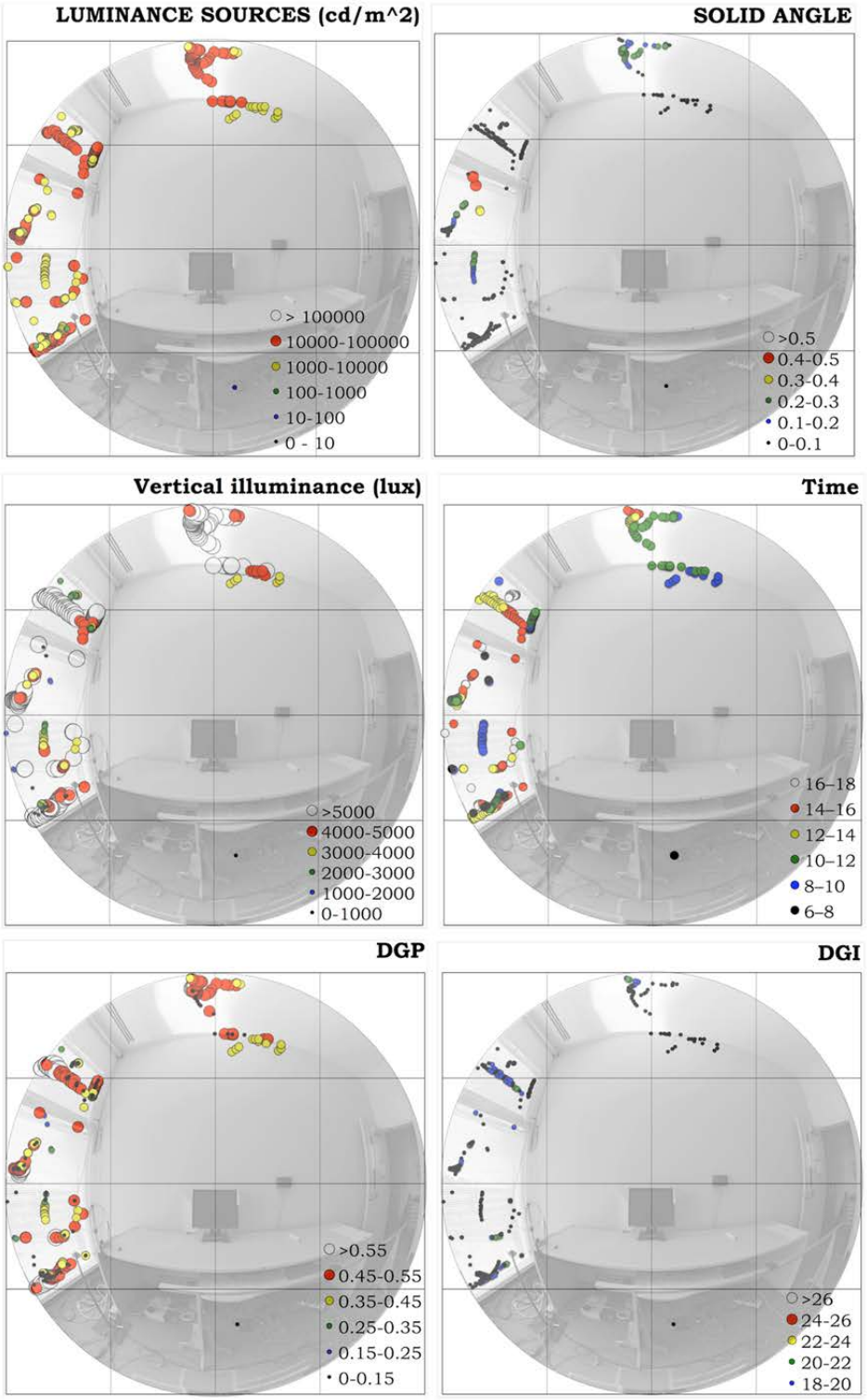

Fig. 22. A: Luminance of glare sources (cd/m^2), B: size of glare sources (st), C: range of vertical illuminance (lux) for the identified glare sources; D: time of day when the glare occurred, E: DGP associated with the glare sources, F: DGI associated with the glare sources. Data are given for the P1 system looking toward the west sidewall on March 12, 2013 under clear sky conditions. The lower

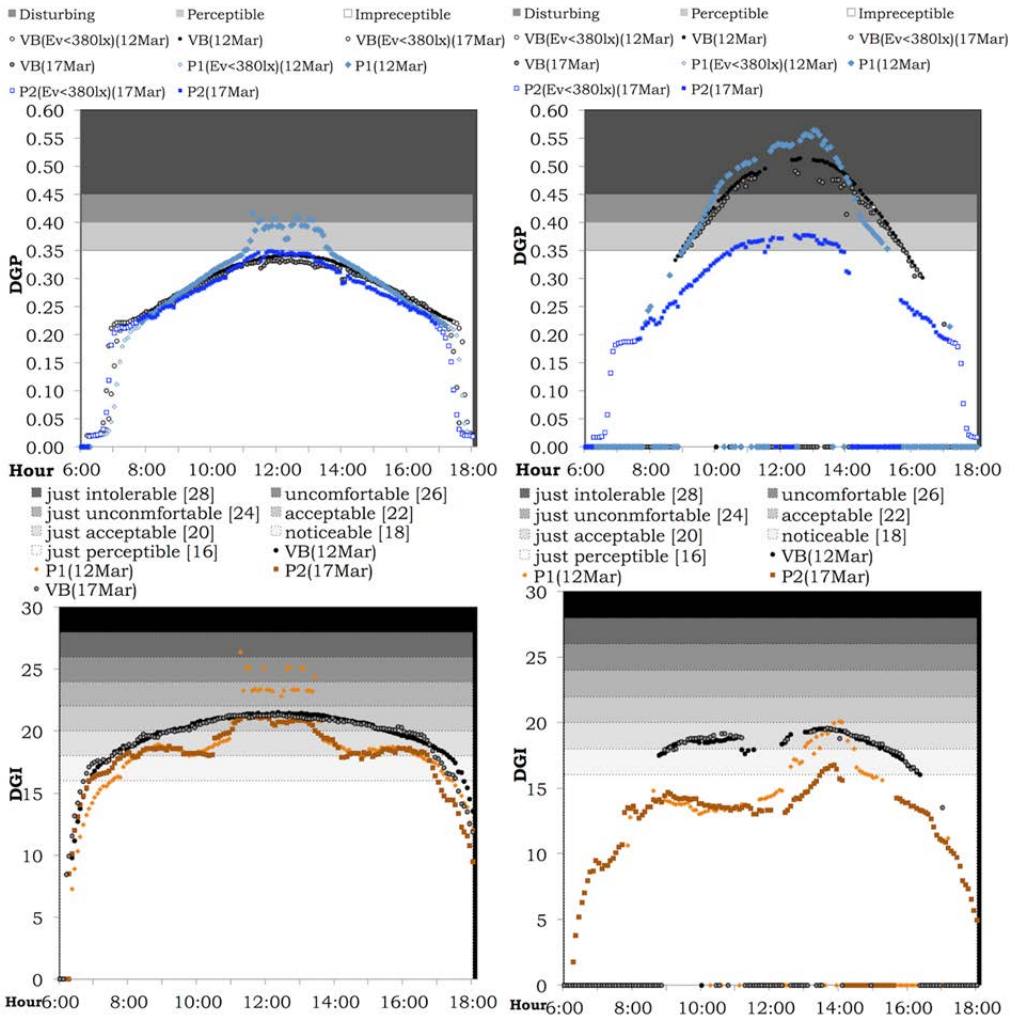

Fig. 23. Daylight glare probability (DGP, upper row) and daylight glare index (DGI, lower row) versus time of day computed using *evalglare* for three systems (VB, P1 and P2) on clear sunny equinox days with daylight from both the upper and lower windows. Left column: View of the window from the back of the room. Right column: View from the center of the room looking at the west wall. Measurements were done on March 12, 2013 (VB and P1) and March 17, 2013 (VB and P2). The lower window was shaded by a Venetian blind in both the reference and test rooms.

The workplane illuminance data can be interpreted in two ways, given that the levels were measured in a relatively shallow space (4.6 m deep (15 ft)): a) lighting energy savings are likely to be significantly improved for shallow perimeter zones because indoor shades covering conventional windows are typically not adjusted to optimize for daylight and because the reference case assumed a non-conservative cut-off slat angle which produced more daylight but also more glare – the reference blind would likely be more closed, and b) lighting energy savings are likely to extend deeper into the perimeter zone, particularly during winter periods (for this south-facing façade), given that the monitored daylight levels at the 3.8 m depth (12 ft) were significantly above the setpoint level of 500 lux. A companion simulation study (McNeil et al. 2013) quantifies annual lighting energy savings in a deep open plan office zone, indicating that the conventional rule of thumb that defines a daylit zone (i.e., 1-1.5 times the head height of the window) could be amended to 2 or perhaps 3 times the head height of the window for this type of technology, depending on the design details of the zone (e.g., surface reflectances,

height of partitions, etc.) and criteria for percentage of year that daylight autonomy is achieved. Additional monitored field studies in deeper spaces are needed.

In order to reduce lighting energy use, a dimmable lighting control system will need to be installed. Because sunlight is redirected towards the ceiling, a shielded photosensor with a downward looking view of the horizontal work plane will provide the most reliable control. Photosensors with a view toward the window wall should not be used. Impact on window heat gains and HVAC energy use was not evaluated. The P1 and P2 systems will require an unshaded clerestory aperture (although the window area is small) and will result in more solar heat gains than a shaded window with a conventional interior blind. The P2 system also involves two films on surfaces #2 and #3, so sputtered low-e coatings cannot be used to control window heat gains unless the film itself can be imbued with low-emittance properties. HVAC impacts should be evaluated in future studies.

Aesthetics were evaluated anecdotally. Unlike reflective prismatic films, which can cause strong patterns of bright light on room surfaces, patterns of redirected sunlight from the P1 and P2 refractive prismatic films were fairly uniform. There were slight variations of light and dark when the incident sunlight was at a more oblique angle to the window but with the addition of daylight from the lower window, these may be rendered unnoticeable when ambient lighting levels in the room are increased. Examples of such patterns can be seen in Fig. 17 (but note that photographs can portray greater contrast than that perceived by the eye).

Outdoor view is not possible through the film. With the addition of the lower view window, occupant requirements for view may be satisfied. The daylighting systems do provide information about the outdoor weather conditions. Daylight levels and the luminance patterns within the room will vary over the course of the day and with variable sky conditions. Chromatic dispersion or rainbow effects occurred with the P1 system which could be perceived positively by occupants.

These systems are designed to daylight an indoor space that has minimal vertical obstructions (for example, open plan furniture with partition heights of less than 1.8 m (6 ft)) from south-, east-, and west-facing clerestory windows (in the Northern Hemisphere) with a sill height that keeps redirected sunlight out of the eyes of the occupants (for example, 1.8 m above the floor). The ceiling is assumed to have a high reflectance (for example, white matte paint with Rvis greater than 0.80) so that the redirected daylight on the ceiling can be reflected to the point of use. The façade should have minimal obstructions on the outside. Overhangs, deep recessed windows, trees, and nearby buildings will reduce the energy-efficiency performance of the system. For retrofit applications, clear glazed windows with a high visible transmittance will perform better than those with dark tinted glass.

The films were tested over a two-year period and subjected to frequent handling (the panel was taken out and put back in every two weeks as other test conditions unrelated to this study were evaluated) and to normal levels of dust and dirt. The systems were never cleaned over the course of the monitored period. If the film is adhered to the indoor window surface as a retrofit measure, the film would require special instructions for cleaning to avoid damaging the prismatic microstructures.

5. Conclusions

Microstructured prismatic daylighting films can be manufactured using roll-to-roll fabrication methods. These films can be adhered to the indoor face of existing glazing as a retrofit measure or adhered within an insulating glazing unit to protect the film from dust and dirt. The films are designed to refract sunlight to the ceiling plane and can be a low-cost alternative to macroscopic daylighting systems such as light shelves. The particular prismatic film evaluated in this study consists of four-sided asymmetrical prismatic protrusions with a height between 50-250 micrometers and an overall index of refraction of 1.5.

A monitored field test was conducted in a full-scale office testbed to evaluate the daylighting performance of two daylight redirecting systems relative to a conventional shaded window. The first system ("P1") consisted solely of the prismatic film. The second system ("P2") combined the prismatic film with a diffusing film in an insulating glazing unit. The diffusing film retained the directionality of the outgoing light but spread the light in a small outgoing range of angles. Measurements of workplane illuminance and field-of-view luminance were taken at regular intervals over a two-year period. Analysis of discomfort glare was conducted using high dynamic range images processed with the *evalglare* software tool, which computes the daylight glare probability (DGP) and other metrics used to evaluate visual discomfort.

We found that the P1 system resulted in perceptible levels of discomfort glare while the P2 system controlled glare to imperceptible levels over the course of clear sunny days from the most conservative view point in the rear of the room looking toward the window. Daylight illuminance levels at the rear of the 4.6 m (15 ft) deep room were significantly increased above the reference window condition, which was defined as the same glazed clerestory window but with an interior Venetian blind (slat angle set to the cut-off angle), for the equinox to winter solstice period on clear sunny days. For partly cloudy and overcast sky conditions, daylight levels were improved slightly.

The prismatic film provides a near-term, potentially low-cost solution for daylighting perimeter zones, particularly for sunny climates and facades with a high degree of exposure to direct sunlight. Case study installations of the film have been conducted by the manufacturer in full-scale occupied buildings under the US Department of Defense Environmental Security Technology Certification Program (ESTCP 2013) and other utility demonstration programs. Results from these additional studies are expected to complement this detailed monitored field study by providing long-term subjective response data.

Acknowledgments

We would like to thank Raghunath Padiyath and Doug Huntley at the 3M Company for their in-kind contributions of time and material and our LBNL colleagues Dennis DiBartolomeo, Howdy Goudey, Daniel Fuller, and David Parker for their technical support throughout the duration of this project.

This work was supported by the Assistant Secretary for Energy Efficiency and Renewable Energy, Building Technologies Program, of the U.S. Department of Energy, under Contract No.

DE-AC02-05CH11231 and by the California Energy Commission through its Public Interest Energy Research (PIER) Program on behalf of the citizens of California.

References

Bartenbach C, Möeller M, Lanzenberger R. Arrangement for illuminating a room with daylight, US Patent 4,699,467, October 13, 1987.

Beltrán LO, Lee ES, Selkowitz SE. 1997. Advanced optical daylighting systems: Light shelves and light pipes. *Journal of the Illuminating Engineering Society* 26(2):91-106.

Clear RD. 2013. Discomfort glare: What do we actually know? Lighting Research and Technology 45 (2013):141-158.

D&R International, Ltd. 2012. Buildings Energy Data Book, Table 1.1.5, p. 1-3 and Table 3.1.5, p. 3-3. Prepared by: D&R International, Ltd. under contract to Pacific Northwest National Laboratory 2012 for the US Department of Energy, Office of Energy Efficiency and Renewable Energy, Building Technologies Program. Washington, DC. http://buildingsdatabook.eren.doe.gov/

ESTCP. 2013. US Department of Defense Environmental Security Technology Certification Program (ESTCP), http://www.serdp.org/Program-Areas/Energy-and-Water/Energy/Conservation-and-Efficiency/EW-201014/EW-201014/(language)/eng-US#factsheet-6986-objective, accessed April 9, 2013.

Hirning MB, Isoardi GL, Coyne S, Garcia Hansen VT, Cowling I. 2013. Post occupancy evaluations relating to discomfort glare: A study of green buildings in Brisbane. Building and Environment 59 (2013): 349–357.

Hopkinson RG, Bradley RC. 1960. Glare from Very Large Sources, Illuminating Engineering (55): 288-297.

Illuminating Engineering Society of North America, ANSI/ IESNA RP-1, American National Standard for Office Lighting, 2004.

Mardaljevic J, Fan D. 2010. HDRcapOSX *http://www.iesd.dmu.ac.uk/~jm/doku.php?id=resources:hdrcaposx,* accessed August 16, 2013.

McNeil A, Lee ES, Jonsson JC. 2013. Daylight performance of a microstructured prismatic window film in deep open plan offices. To be submitted to Solar Energy.

Moench J, Rentzsch H, Lang G, Mueller H. Device for guiding daylight, US Patent 4,654,243 (Siemens), March 31, 1987.

Padiyath R. Hybrid Light Redirecting And Light Diffusing Constructions, pending US Patent Application Serial Number 61/469147, filed March 30, 2011.

Padiyath R, Marttila C, Nestegard M. Light redirecting constructions, US Patent Publication 2013/0038928 A1, February 14, 2013.

Reinhard E, Ward G, Pattanaik S, Debevec P. High Dynamic Range Imaging: Acquisition, Display, and Image-Based Lighting, Morgan Kaufmann Publishers, San Francisco, 2005.

Ruck N, Aschehoug O, Aydinli S, Christoffersen J, Courret G, Edmonds I, Jakobiak R, Kischkoweit-Lopin M, Klinger M, Lee E, Michel L, Scartezzini JL, Selkowitz S. 2000. Daylight in buildings: A source book on daylighting systems and components. http://gaia.lbl.gov/iea21/

Shehabi A, DeForest N, McNeil A, Masanet E, Lee ES, Milliron D. 2013. US energy savings potential from dynamic daylighting control glazings. Energy and Buildings 66 (2013): 415-423.

Van Den Wymelenberg KG, Inanici MN, Johnson PW. 2010. The Effect of Luminance Distribution Patterns on Occupant Preference in a Daylit Office Environment. Leukos 7(2): 103–122.

Wadsworth F. Illuminating prism structure, US Patent 720,386, February 10, 1903.

Ward G. 2009. *hdrcaposx* software, originally developed for LBNL by Anyhere Software, http://www.anyhere.com/, accessed August 16, 2013.

Ward G. 2009. Radiance *hdrgen* tool, http://www.anyhere.com/, accessed August 16, 2013.

Wienold J, Christoffersen J. 2006. Evaluation methods and development of a new glare prediction model for daylight environments with the use of CCD cameras, *Energy and Buildings* 38(7):734-757.

Wienold J. Dynamic daylight glare evaluation, Building Simulation 2009, 11th International IBPSA Conference, Glasgow, Scotland, July 27-30, 2009.

Wienold J. 2009. Workshop: Glare analysis of HDR images. Presentation at the 8th Radiance Workshop, Boston, MA, October 21, 2009, http://www.radiance-online.org:82/radiance-workshop8/Presentations/wienhold_rad_ws_2009_glare_intro.pdf, accessed August 13, 2013.

Wienold J. *evalglare* version 1.0, September 2012, Fraunhofer Institute for Solar Energy Systems, Freiburg, Germany.